

AD-A250 220



DTIC  
ELECTE  
MAY 19 1992  
S C D

4  
(2)

Final Technical Report  
for  
AFOSR Grant No. 89-0201

AFOSR-TR- 92 0306

**HIGH TEMPERATURE DEFORMATION PROCESSES AND STRENGTHENING  
MECHANISMS IN INTERMETALLIC PARTICULATE COMPOSITES**

Submitted to :

Department of the Air Force  
Directorate of Electronic and Materials Sciences  
Air Force of Office of Scientific Research  
Bolling Air Force Base, Building 410  
Washington D.C. 20332

Attention: Dr. Alan Rosenstein

Submitted by:

Professor William D. Nix, Principal Investigator  
Department of Materials Science and Engineering  
Stanford University, Stanford, CA 94305

**92-12948**



March 1992

Department of MATERIALS SCIENCE AND ENGINEERING

STANFORD UNIVERSITY

**92 5 14 060**

Approved for public release;  
distribution is unlimited.

REPORT DOCUMENTATION PAGE			Form Approved OMB No. 0704-0188	
Public reporting burden for this collection of information is estimated to average 1 hour per response, including the time for reviewing instructions, searching existing data sources, gathering and maintaining the data needed, and completing and reviewing the collection of information. Send comments regarding this burden estimate or any other aspect of this collection of information, including suggestions for reducing this burden, to Washington Headquarters Services, Directorate for Information Operations and Reports, 1215 Jefferson Davis Highway, Suite 1204, Arlington, VA 22202-4302, and to the Office of Management and Budget, Paperwork Reduction Project (0704-0188), Washington, DC 20503.				
1. AGENCY USE ONLY (Leave blank)		2. REPORT DATE March 31, 1992	3. REPORT TYPE AND DATES COVERED Final Technical Report 12/88 - 12/91	
4. TITLE AND SUBTITLE High Temperature Deformation Processes and Strengthening Mechanisms in Intermetallic Particulate Composites			5. FUNDING NUMBERS AFOSR No. 89-0201	
6. AUTHOR(S) William D. Nix, Keith R. Forbes and D. D. Sternbergh				
7. PERFORMING ORGANIZATION NAME(S) AND ADDRESS(ES) The Department of Materials Science and Engineering Stanford University 125 Panama, Jordan Quad/Birch Stanford, CA 94305-4125			8. PERFORMING ORGANIZATION REPORT NUMBER AFOSR - 92-1	
9. SPONSORING/MONITORING AGENCY NAME(S) AND ADDRESS(ES) AFOSR/NE Building 410, Bolling AFB DC 20332-6448			10. SPONSORING/MONITORING AGENCY REPORT NUMBER F49620-92-J-0009	
11. SUPPLEMENTARY NOTES ATTN: Dr. Alan H. Rosenstein				
12a. DISTRIBUTION/AVAILABILITY STATEMENT  APPROVED FOR PUBLIC RELEASE; DISTRIBUTION IS UNLIMITED.			12b. DISTRIBUTION CODE	
13. ABSTRACT (Maximum 200 words)  Research on the high temperature deformation processes and strengthening mechanisms in Intermetallic Particulate Composites is described. Work of the grant included high temperature compression tests of $\text{Ni}_3\text{Al} - \text{Al}_2\text{O}_3$ composites; mechanical alloying of $\text{Ni}_3\text{Al} + \text{Y}_2\text{O}_3$ ; transient deformation studies of the intermetallics $\text{Ni}_3\text{Al}$ , $\text{NiAl}$ , and $\text{NiBe}$ ; and development of a model of dislocation structure control of plastic deformation. Work during the past year on the high temperature deformation of $\text{NiAl}$ single crystals is also described.				
14. SUBJECT TERMS  Intermetallic Alloys, High Temperature Strength			15. NUMBER OF PAGES 42	
			16. PRICE CODE	
17. SECURITY CLASSIFICATION OF REPORT  UNCLASSIFIED	18. SECURITY CLASSIFICATION OF THIS PAGE  UNCLASSIFIED	19. SECURITY CLASSIFICATION OF ABSTRACT  UNCLASSIFIED	20. LIMITATION OF ABSTRACT	

Final Technical Report  
for  
AFOSR Grant No. 89-0201

**HIGH TEMPERATURE DEFORMATION PROCESSES AND STRENGTHENING  
MECHANISMS IN INTERMETALLIC PARTICULATE COMPOSITES**

Submitted to :

Department of the Air Force  
Directorate of Electronic and Materials Sciences  
Air Force of Office of Scientific Research  
Bolling Air Force Base, Building 410  
Washington D.C. 20332

Attention: Dr. Alan Rosenstein

Submitted by:

Professor William D. Nix, Principal Investigator  
Department of Materials Science and Engineering  
Stanford University, Stanford, CA 94305

Accession For	
NTIS Grant	<input checked="" type="checkbox"/>
NTIS TAB	<input type="checkbox"/>
Unannounced	<input type="checkbox"/>
Justification	
By	
Distribution/	
Availability Codes	
Dist	Avail and/or Special
A-1	

March 1992

This research was supported by the Air Force of Scientific Research (AFOSC) under Grant No. AFOSR-89-0201. Approved for public release; distribution unlimited.

Qualified requesters may obtain additional copies from the Defense Documentation Center; all others should apply to the Clearing House for Federal Scientific and Technical Information.



## Table of Contents

<b>Summary.....</b>	<b>1</b>
<b>I. Development of Experimental Techniques</b>	
A. Development of an Improved High Temperature Compression Test Apparatus .....	2
<b>II. Deformation Mechanisms in Intermetallic Alloys</b>	
A. Description of Deformation in Ni <sub>3</sub> Al.....	4
B. Transient Deformation in Polycrystalline B2 Intermetallics.....	11
C. High Temperature Deformation of Single Crystal NiAl.....	15
<b>III. Particle Strengthening of Intermetallic Alloys</b>	
A. High Temperature Compression Tests of Ni <sub>3</sub> Al-Al <sub>2</sub> O <sub>3</sub> Composites.....	30
B. High Temperature Comprerssion Tests of Ni <sub>3</sub> Al-Y <sub>2</sub> O <sub>3</sub> Particulate Composites.....	34
<b>IV. Oral Presentations Resulting from AFOSR Grant No. 89-0201.....</b>	<b>40</b>
<b>V. Publications Resulting from AFOSR Grant No. 89-0201.....</b>	<b>41</b>
<b>VI. Ph.D. Students Supported by AFOSR Grant No. 89-0201.....</b>	<b>42</b>

## Summary

We have conducted a fundamental study of the high temperature deformation processes and strengthening mechanisms in intermetallic systems, supported under AFOSR Grant No. 89-0201. In this report we describe the results of this three-year effort.

Intermetallic compounds offer many advantages for high temperature structural applications over current materials conventionally used for these purposes. They tend to have lower densities, their complex crystallographic configurations make deformation more complex and difficult and offer alloying possibilities which are both intriguing and promising. The aim of our research has been to study and understand the deformation processes and strengthening mechanisms that operate in intermetallic particulate composites at high temperatures, studying both two-phase materials with some work in single phase intermetallic alloys.

In order to elicit insights into the details of their behavior, we have had to develop improved apparatus and techniques for testing at high temperatures. We have developed the capability to perform tests with high spatial and time resolution at high temperatures. This has proven useful in studying the transient behavior of these materials, the responses to sudden changes in testing conditions which allow us to distinguish between the contributions of various deformation mechanisms. We are now able to develop tests which incorporate a wide variety of transients in unlimited combinations.

Our study is grounded on our investigations into the fundamental behavior of nickel-based intermetallics, covering polycrystalline beryllides and aluminides as well as single crystal NiAl and Ni<sub>3</sub>Al. We have studied these materials in the high temperature range (i.e. beyond the peak in yield strength of Ni<sub>3</sub>Al) both in tension creep and in compression under controlled strain rate. These tests have demonstrated the intrinsic difficulty of dislocation glide under these conditions, and its importance to high temperature strength. Glide, however, is not the sole controlling factor; the dislocation substructure is also very important. The two interact in complex ways which make these materials a challenge to characterize.

Finally, we have studied Ni<sub>3</sub>Al in particulate composites. Composites containing high volume fractions of Al<sub>2</sub>O<sub>3</sub> have been shown to retain strength right up to the melting temperature of the Ni<sub>3</sub>Al phase. Polycrystalline Ni<sub>3</sub>Al with dispersoids of Y<sub>2</sub>O<sub>3</sub> retain ultra-fine grain structures which show significant plasticity in compression, with strengths comparable to other fine grained superalloys. The deformation characteristics, however, reflect the complex interaction of intrinsically difficult glide and dislocation substructure.

## **I. Development of Experimental Techniques**

### **A. Development of an Improved High Temperature Compression Test Apparatus.**

K.R. Forbes and D.D. Sternbergh (Graduate Research Assistants)

Our investigation of deformation processes in intermetallic compounds has included both steady state and transient testing. The effectiveness of these tests depends upon the accuracy in measuring the parameters of the experiment: strain, stress, and temperature. The need for accurate strain measurements is especially necessary in the transients of strain rate change tests and stress relaxation tests. One of the experimental challenges of the research has been to determine accurately the plastic strain rate during an experiment. This is complicated by the high temperatures at which tests must be performed. Typically displacements are measured at the crosshead far away from the sample and the machine constant is determined in order to find the strain at the sample. This procedure requires that the spring constant of the machine be known accurately in order to obtain good data. This spring constant must be determined in a separate experiment and still is only approximate and variable, especially at low loads. Errors of 10% to 20% are typical and are sufficient to result in spurious strain rate data, to the extent that strain rate discontinuities can be measured where such are not possible. [1, 2]

To correct these inaccuracies, we have designed and built an apparatus which measures displacement directly at the sample and circumvents the machine linkage and thus the errors it produces. Measuring strain at the sample is especially difficult at high testing temperatures. Measuring devices are not stable at these temperatures and the displacement at the sample must be translated to displacements at a more suitable position. We accomplish this by connecting alumina rods and tubes to the platens next to the sample in the set-up illustrated in Figure 1. The inner rod is fixed to the upper platen and slides freely in the outer tube which is secured to the bottom platen. Relative displacement of the platens, which is exactly the change in length of the sample, is transferred to the other end of the tubes and rods. At this end a linear variable displacement transducer (LVDT) is connected and the length of the sample measured at any point in time. The LVDT is water cooled to a constant temperature at which it has been calibrated. The rods from the furnace are allowed to equilibrate to the imposed temperature gradient so that thermal expansion effects are negated.

This set-up has been effectively utilized at temperatures as high as 1400° C. Displacement measurements are accurate to within 5  $\mu\text{m}$ . Hardware development has been augmented with new control and acquisition software. As a result, true strain rate control and accurate strain measurements are achieved, even at elevated temperatures.

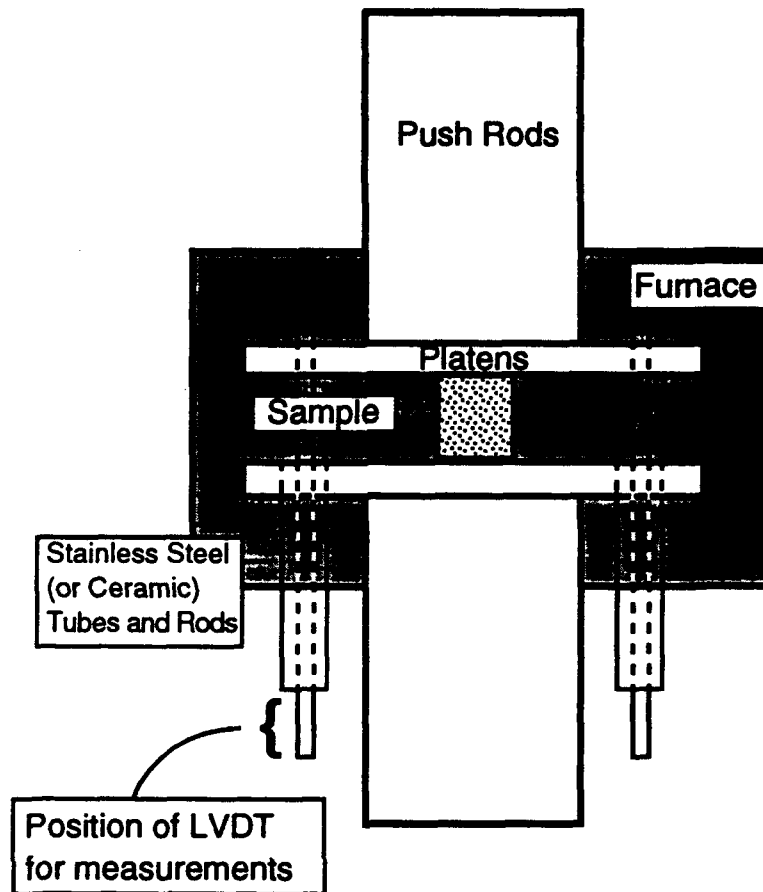


**Figure 1:** Various elements of the high temperature compression test apparatus.

### References

1. Deborah Lynn Yaney, Ph.D. Dissertation, Stanford University (1986).
2. J.C. Gibeling, J.H. Holbrook and W.D. Nix, *Acta Metall.*, 32, 1287 (1984).

## II. Deformation Mechanisms in Intermetallic Alloys

### A. Description of Deformation in Ni<sub>3</sub>Al

#### Glide of Dislocations in Ni<sub>3</sub>Al

The high temperature strength of intermetallic compounds with the L1<sub>2</sub> crystal structure has attracted a great amount of attention in recent years. Interest in these materials is related to their unusual ability to become stronger with increasing temperature. This phenomenon, called the yield strength anomaly, has stimulated both scientific study and technological development. The yield strength anomaly of Ni<sub>3</sub>Al has been studied extensively and it is generally accepted that the increase in the critical resolved shear stress (CRSS) with temperature involves primary octahedral glide which is retarded by "cross-slip" onto the (010) plane. By comparison, very little attention has been paid to the creep properties of Ni<sub>3</sub>Al. It has been observed [1,2] that the creep strength of Ni<sub>3</sub>Al decreases with increasing temperature in the region where the CRSS increases with temperature, but the dislocation mechanisms that control the creep behavior have only recently been identified [2]. It has been shown that octahedral glide is exhausted during primary creep and that most of the creep deformation following this exhaustion process is caused by the bowing out and gliding of dislocations on the (010) cube cross-slip plane. The observation of octahedral glide during primary creep suggests that yielding and primary creep are related processes.

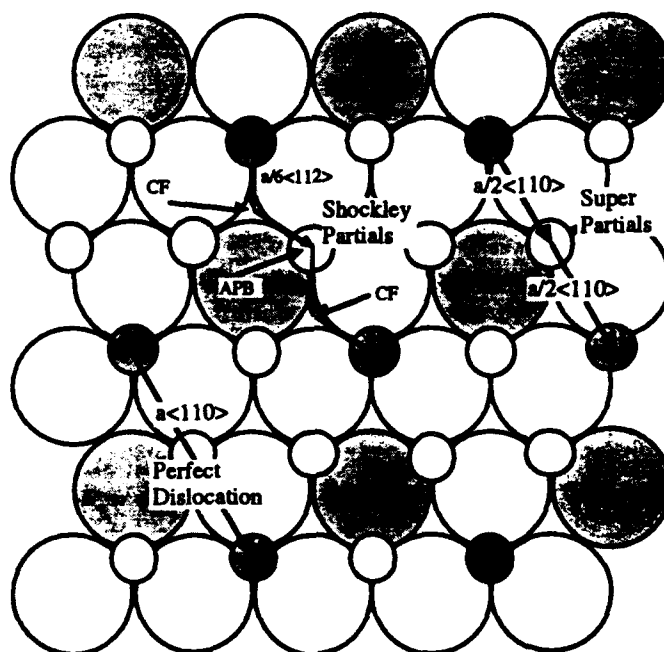


**Figure 1:** The octahedral plane for the L1<sub>2</sub> crystal structure. The small atoms are out of the page. Notice that superpartial dislocations place atoms next to the wrong neighboring atoms and produce an APB. Shockley partial dislocations lead to the formation of a CSF that includes both an APB and a stacking fault.



The L1<sub>2</sub> ordered structure for Ni<sub>3</sub>Al is an FCC derivative. The glide planes for Ni<sub>3</sub>Al, the octahedral planes, are the same as for ordinary FCC metals, but a unit dislocation in the ordered structure has a Burgers vector that is twice as large as a unit dislocation in FCC (see Fig. 1). The strain energy associated with this large dislocation causes it to dissociate into two "super-partial" dislocations and this leads to the formation of an anti phase boundary (APB). Each super-partial dislocation will in turn dissociate into two Shockley partial dislocations that are connected by a complex stacking fault (CSF) on the octahedral plane (Fig. 1). It follows that the core of a super dislocation in Ni<sub>3</sub>Al is actually a planar, ribbon-like structure containing four partial dislocations that are connected by an APB and two CSFs.

Octahedral glide in Ni<sub>3</sub>Al is an easy glide process as long as the dislocation core lies on the octahedral plane; however, dislocations do not always remain on the octahedral plane. Yoo<sup>[3]</sup> has shown that for Ni<sub>3</sub>Al there is a torque (caused by the anisotropic elastic interactions of the super dislocations) that promotes cross slip onto the (010) cube cross slip plane. Yielding experiments on single crystals of Ni<sub>3</sub>Ga by Takeuchi and Kuramoto<sup>[4]</sup> and Ni<sub>3</sub>Al by Pope et al.<sup>[5-7]</sup> have shown that this cross slip event is dependent on the orientation of the applied stress. The observed orientation dependence indicates that the constriction of the leading Shockley partials by an Escaig type force and the resolved shear stress on the cube plane are both important factors that contribute to the frequency of the cross slip event. When the screw segment of a dislocation is fully cross slipped, the movement of that dislocation segment becomes a difficult processes.

The cross slip of dislocations from the (111) plane (where they are mobile) to the (010) plane (where they are immobile) is the basis for the increase in yield strength with temperature that is observed for Ni<sub>3</sub>Al. Cross slip is a thermally activated process, and the probability of this cross slip event increases with increasing temperature. Since the cross slip event impedes octahedral glide, it follows that dislocation motion on the octahedral plane becomes increasingly more difficult at higher temperatures. The fact that dislocation motion becomes more difficult at higher temperatures translates to an increase in strength and accounts for the anomalous yielding behavior of this alloy.

Various models have been proposed to explain the exact mechanism by which the formation of a cross slipped dislocation segment leads to the observed increase in flow stress in Ni<sub>3</sub>Al. We have performed temperature change, stress relaxation and exhaustion/temperature reduction experiments on Ni<sub>3</sub>Al and interpreted the results as they relate to various proposed models for deformation.

#### Cottrell-Stokes Type Experiments

The effects of dislocation mobility and dislocation substructure on the flow properties of a material can be evaluated by the use of a temperature change test that was first proposed by Cottrell and Stokes<sup>[8]</sup>. Mobility controlled dislocation glide is a dynamic process wherein a change in temperature during a yielding experiment will result in an immediate change in the flow stress. For mobility controlled deformation, the change in the flow stress is immediate because the processes that control mobility are reversible processes. For

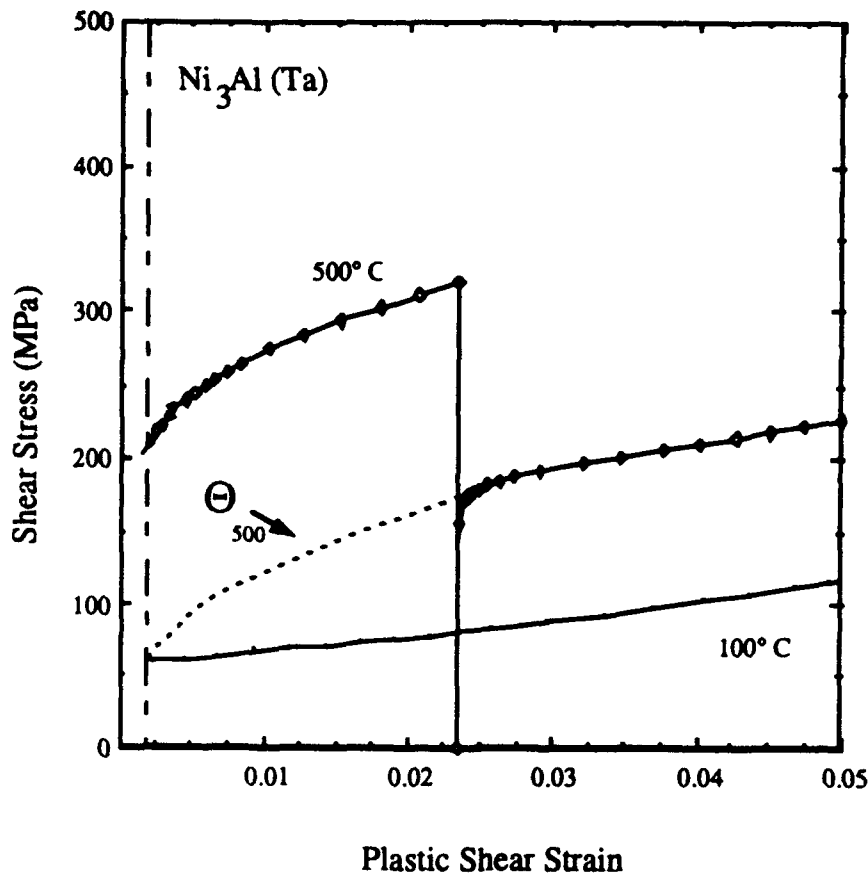


**Figure 2:** The results of a Cottrell-Stokes type test on  $\text{Ni}_3\text{Al}$ . The flow stress after the temperature change is shown to be both: dependent on strain hardening, and a partially reversible process.

dislocation motion that is substructure controlled, changing the temperature without changing the structure will not lead to an immediate change in the flow stress. In this case, dislocation glide is not a recoverable process because the formation of the dislocation substructure is not reversible.

The proposed yielding models for  $\text{Ni}_3\text{Al}$  can be classified as either mobility controlled or structure controlled processes and can therefore be examined by Cottrell-Stokes type experiments. The cross slip pinning model predicts that an equilibrium number of pinning points exists at a given temperature and that the formation and annihilation of pinning points is completely reversible with temperature. In contrast to the cross slip pinning model, the superkink model and the percolation model are very dependent on structure and do not include a reversible process.

We have performed Cottrell-Stokes type temperature change yielding experiments to determine if octahedral glide in  $\text{Ni}_3\text{Al}$  is a reversible process. Monotonic tests were conducted at 100° and 500° C and a temperature change test was run such that the specimen was strained 2% at 500° C, unloaded, and then reloaded at 100° C. It was expected that if dislocation motion were structure dependent that the flow stress would return to its value at

500° C, but that if dislocation glide were reversible it would drop to the value measured in the 100° C monotonic test.

The results obtained from the Cottrell-Stokes type experiment are shown in Fig. 2. As is shown in the figure, the value of the flow stress after the temperature change is equal to the sum of the 100° C yield stress and the change in stress caused by strain hardening at 500° C. It was concluded that the "harder" structure introduced at 500° C influences the subsequent deformation at 100° C, but that the processes that control deformation are also partially reversible.

The experiment conducted in this study is similar to the experiments conducted by Stoloff and Davies<sup>[9]</sup> and Dimiduk<sup>[10]</sup>, and the results of this work are in agreement with the results of the others. Stoloff and Davies and Dimiduk have chosen to discount the effects of strain hardening and have interpreted their results as an indication that yielding in Ni<sub>3</sub>Al is a completely reversible process. Ignoring the effects of strain hardening altogether can be questioned; as can be seen in Fig. 1, the anomalous strain hardening rate has an important effect on the measured 0.2% offset yield stress. For this reason we have included the effects of strain hardening in our study. The difference between partial and fully recoverable flow will be addressed in greater detail in the discussion of the stress relaxation / temperature drop experiments.

### **Stress Relaxation Experiments.**

Materials in which flow is controlled by dislocation mobility are generally acknowledged to be very strain rate sensitive and are usually characterized by a large strain rate exponent ( $m$ ) and a low stress exponent ( $n$ ). However, the effect of strain rate on the flow stress of Ni<sub>3</sub>Al as measured in constant strain rate experiments has been shown to be negligible<sup>[11]</sup>. In order to determine if dislocation mobility plays an important role in determining the flow stress, stress relaxation experiments have been conducted to measure the effects of stress and strain rate on the flow properties of Ni<sub>3</sub>Al.

The stress exponent ( $n$ ) and the activation volume ( $V_{act}$ ) are deformation parameters that can be used to identify the microstructural mechanisms that control deformation. Materials in which dislocation mobility controls deformation (i.e. solid solution alloys and bcc metals) typically have values of  $n$  near 5 and  $V_{act}$  of about  $100 b^3$ . By comparison, materials in which deformation is controlled by the dislocation substructure, (i.e. pure fcc metals and Class II solid solution alloys) values for  $n$  and  $V_{act}$  are closer to 100 and  $2000 b^3$  respectively.

The curve given in Fig. 3 (a) is representative of the stress relaxation curves that were obtained in this study. The observation that the strain rate drops to a very low value with very little change in stress suggests that dislocations are immobilized very quickly. We believe this occurs by the formation of KW locks. As is shown in Fig. 3 (b), the stress exponent ( $n$ ) for Ni<sub>3</sub>Al was determined to be 200. Comparing this value with the materials listed in Table II suggests that deformation of Ni<sub>3</sub>Al should not be considered as dislocation mobility controlled but rather should be considered dislocation obstacle

controlled. This “pure metal like” behavior suggests that a small number of highly mobile dislocations carry the deformation and that most of the dislocations are sessile and are a part of the dislocation substructure, *i.e.* in the form of KW locks.

Stoiber *et al.* [12] have conducted similar stress drop experiments in order to determine the activation volume of Ni<sub>3</sub>Al. Results from their work indicate that the activation volume for Ni<sub>3</sub>Al (1% Ta) is about 2000  $b^3$ . This value is in good agreement with the experiments that were conducted in the present work, and the results of both stress relaxation experiments suggest that the reversible part of the flow stress is not caused by a reduction of the dislocation mobility, but is instead related to the strain that a dislocation can produce before it cross-slips and forms a KW lock.

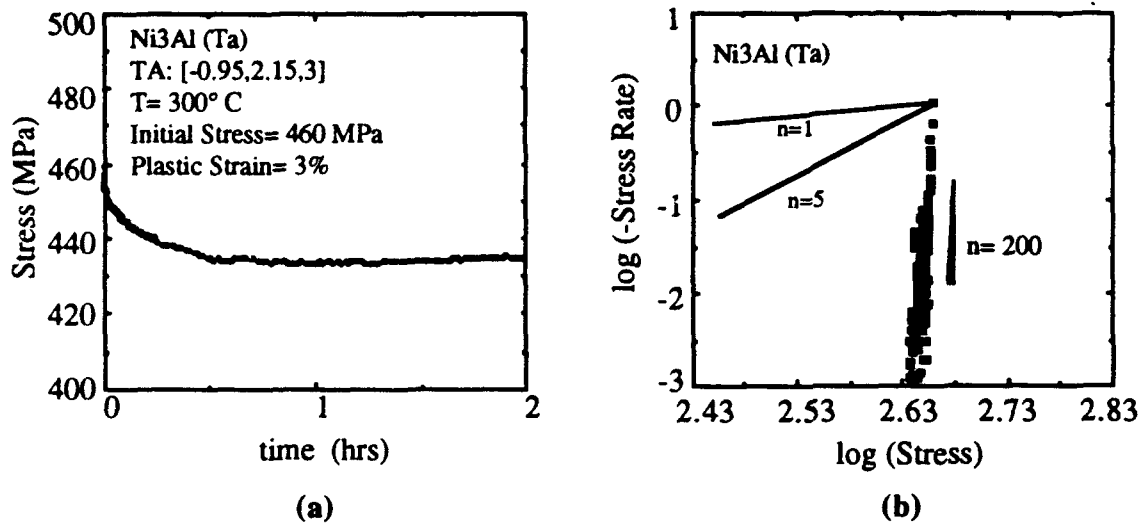


**Figure 3:** (a) A stress relaxation experiment for Ni<sub>3</sub>Al (Ta). The relaxation exhausts after a 6% decrease in stress, and (b) the low temperature stress exponent was determined to be 200.

### Relaxation / Temperature Drop Experiments.

If dislocation motion in Ni<sub>3</sub>Al is a thermally reversible process then the exhaustion observed in the stress relaxation experiments and during primary creep should be reversible. Specifically, a decrease in temperature should bring about an immediate increase in dislocation motion and the observation of additional plastic strain. However, if the dislocation motion in Ni<sub>3</sub>Al is at least partially inhibited by the formation of KW locks, a decrease in temperature will not lead to an increase in dislocation motion because the formation of KW locks is not a reversible process. Reducing the temperature after a stress relaxation experiment, or after the exhaustion of primary creep, without accumulating additional plastic strain could be taken as a strong indication that dislocation motion in Ni<sub>3</sub>Al is only a partially recoverable process and that the formation of KW locks play an important role in determining the flow stress.

A constant strain rate experiment was conducted at 300° C with the specimen being deformed to 2.0 % plastic strain. The cross head was then stopped and the specimen was allowed to relax for 2 hours while the drop in stress was monitored. At this point, the test was switched to constant stress control and the temperature was decreased while the strain was monitored. In a similar experiment, a constant stress of 330 MPa was applied to a creep specimen and the specimen was allowed to deform at 300° C until octahedral glide was exhausted. After this time (24 hours), the furnace was turned off and the strain was monitored as the temperature was allowed to drop. As is shown in Fig. 4 the temperature was reduced by approximately 40° C in the yielding experiment and 30° C in the creep experiment before any change in strain was observed. This drop in temperature without a corresponding increase in strain is taken as an indication that octahedral glide is not a completely recoverable process and that the formation of KW locks during primary creep has an important effect on the flow properties of Ni<sub>3</sub>Al.

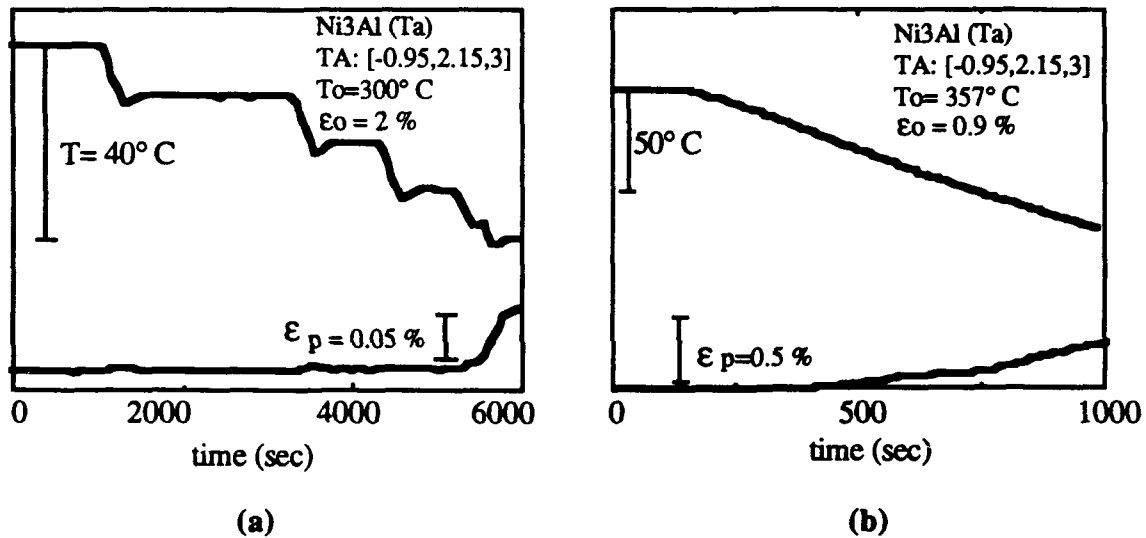


**Figure 4:** Deformation exhaustion / temperature drop experiments associated with (a) stress relaxations, and (b) primary creep. The observed decreases in temperature without a corresponding increase in plastic strain indicates that flow is only a partially reversible process.

### Conclusions:

1. The temperature dependence of the flow stress is caused by both:
  - (i) The effect of temperature on the mobility of dislocations and,
  - (ii) The effect of temperature on the immobilization of dislocations and the formation of dislocation substructure.
2. The results of stress relaxation experiments suggest that the reversible part of the flow stress cannot be described in terms of dislocation mobility but should instead be related to the stochastic motion of a relatively small number of highly mobile dislocations.

3. The description of a critical stress for dislocation motion is not consistent with the observation of either primary creep or micro yielding.
4. The cross slip pinning model predicts the reversibility of dislocation motion but does not account for the additional strengthening due to strain hardening.
5. The superkink model predicts that yielding should be structure dependent and can account for strain hardening, but does not account for the partial reversibility of the flow stress.
6. Primary creep and the shape of the stress strain curve suggest that strain hardening, the formation of KW locks, plays an important role in determining the flow stress.
7. A complete description of octahedral glide that is based on the formation of KW locks must include a provision for the dynamic recovery of these locks.
8. In their present form, the yielding models that have been proposed to explain the yielding behavior of Ni<sub>3</sub>Al are unable to explain all of the transient observations. The "kink source" model is able to explain a number of the transient observations and appears to be the best candidate for further development.

#### References

1. J.R. Nicholls, and R. D. Rawlings, *J. Mater. Sci.*, **12**, 2456, (1977).
2. K.J. Hemker, M.J. Mills, and W.D. Nix, submitted to *Acta Metall.*, (1990).
3. M.H. Yoo, *Acta Metall.*, **35**, 1559, (1987).
4. S. Takeuchi and E. Kuramoto, *Acta Metall.*, **26**, 207, (1978).
5. C. Lall, S. Chin, and D.P. Pope, *Metall. Trans.*, **10A**, 1323, (1979).
6. S.S. Ezz, D.P. Pope, and V. Paidar, *Acta Metall.*, **30**, 921, (1982).
7. V. Paidar, D.P. Pope, and V. Vitek, *Acta Metall.*, **32**, 435, (1984).
8. Cottrell-Stokes
9. R.G. Davies and N.S. Stoloff, *Phil. Mag A*, **9**, 349, (1964).
10. D. Dimiduk, Carnegie Melon University, Phd. Dissertation, (1989).
12. G.R. Leverant, W. Gell, and S.W. Hopkins, *Mater Sci. Eng.*, **8**, 125, (1971).
12. J. Stoiber, J. Bonneville and J.L. Martin, *Proc. 8th ICSMA* Ed: P.O. Kettunen, T.K. Lepistö and M.E. Lehtonen, Pergamon Press, Oxford, (1988).

## B. Transient Deformation in Polycrystalline B2 Intermetallics

Although alloys of  $\text{Ni}_3\text{Al}$  have been more extensively developed, this is not the most promising of ordered intermetallics for use in high temperature applications. With a relatively low melting point ( $1390^\circ\text{C}$ ) and high density ( $7.50\text{ g/cm}^3$ ),  $\text{Ni}_3\text{Al}$  offers only a marginal improvement over current superalloy compositions. The intermetallic  $\text{NiAl}$  has a much lower density ( $5.86\text{ g/cm}^3$ ) and a higher melting temperature ( $1640^\circ\text{C}$ ) which could result in significant improvements over current alloys. However, polycrystalline  $\text{NiAl}$  is extremely brittle at room temperature and will require additional processing and alloying to produce a suitable structural material.  $\text{NiAl}$  exists over a large range of stoichiometry with a relatively constant creep strength which suggests that alloying is feasible to improve its mechanical properties. Whittenberger<sup>[1]</sup> has found that the flow stress of  $\text{NiAl}$  does not vary far from 30 MPa at 1300 K for a range of compositions between 43.9 and 52.7 atomic per cent Al.

Both  $\text{NiAl}$  and  $\text{NiBe}$  have a B2 crystal structure in which each (Al,Be) atom is surrounded by four Ni atoms as shown in Fig. 1. The density of  $\text{NiBe}$  ( $6.40\text{ g/cm}^3$ ) is about 10% more dense than  $\text{NiAl}$  even though the element beryllium is lighter than aluminum. This density increase is a result of beryllium also being a smaller atom than aluminum which allows the Ni atoms which surround it to pack themselves more closely. The passage of a dislocation would include the movement of a Al (Be) atom out of its position and into the next well between Ni atoms. The B2 lattice is an open structure allowing Al (Be) atoms to sit deeply between Ni atoms, suggesting a high lattice friction. Thus we would expect that the mobility of dislocations in  $\text{NiAl}$  and  $\text{NiBe}$  to have a relatively low mobility compared to pure metals. The deformation mechanisms in these intermetallic alloys have been studied using transient strain rate change experiments.

Plastic deformation in metals and alloys can be described in terms of two limiting classes: (i) Class I alloys in which the drag forces on the dislocation constrain deformation, and (ii) Class II metals and alloys which display pure metal-type behavior in which the dislocation structure controls deformation.<sup>[1]</sup> Class I alloys are characterized by solid solution alloys in which solute atoms form an atmosphere around the dislocation core which is dragged along as the dislocation moves. Deformation is controlled, in this case,

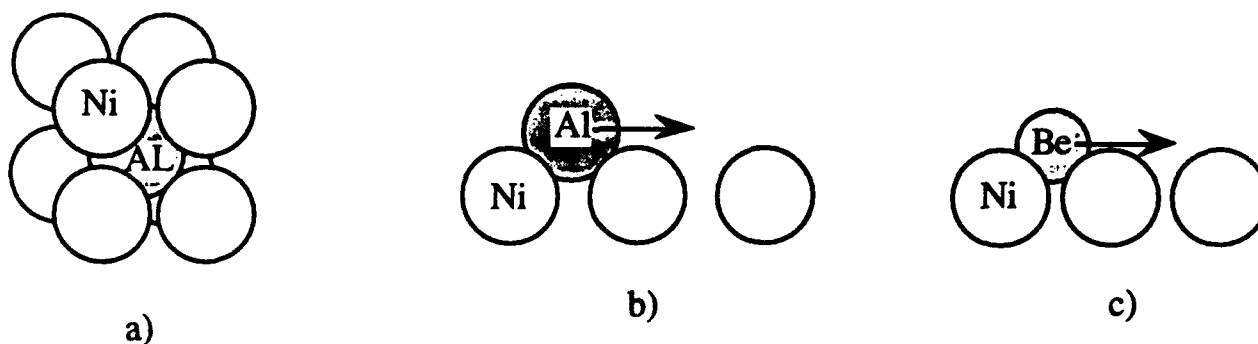


**Figure 1:** a) A unit cell of ordered  $\text{NiAl}$  with the B2 crystal structure. b) An approximation of the relative position of an Al atom in  $\text{NiAl}$  compared with c) that of a Be atom in  $\text{NiBe}$ .

by the diffusion of this solute atmosphere. In pure metals, on the other hand, dislocation motion is not hindered by solute drag, rather dislocations move quickly into a lower energy regular network. A small fraction of the dislocations remain mobile but must cut through the network and thus the structure of this network controls the total deformation.

The different deformation characteristics of Class I and Class II alloys are directly related to the different controlling mechanisms. The transient accompanying a strain rate change can reveal the deformation characteristic of a metal and thus is useful in determining the controlling deformation mechanism. A strain rate change test is accomplished by imposing a constant strain rate until steady state deformation occurs and then increasing or decreasing this strain rate as quickly as possible. A strain rate increase in a Class I alloy must result in an increase in the total number of dislocations which cannot occur instantaneously. The transient response of a Class I alloy is controlled by the time needed to multiply dislocations in a strain rate increase and annihilate them during a rate decrease. As a result, Class I alloys seem initially hard in a strain rate increase but appear soft in the initial transient of a strain rate decrease.

In Class II alloys, the increase in mobile dislocation density needed in a strain rate increase test is readily available with only a small increase in stress and the time for dislocation multiplication is not a limiting factor as with Class I alloys. Thus Class II alloys seem initially weak in a strain rate increase until a hard dislocation structure can be formed. During a strain rate decrease, the hardened structure persists; so that Class II alloys are characteristically strong in a strain rate decrease transient.

Strain rate change tests were performed on the polycrystalline NiAl and NiBe in this investigation in order to characterize the operative dislocation mechanisms. NiAl and NiBe ingots were provided by the Research and Development Division of the Lockheed Missiles and Space Company and cylindrical samples were electron discharge machined to diameter of 4.5 mm and 9 mm length. Compression tests were performed in a computer-controlled Instron testing machine with the test apparatus described in Section A. Constant strain rate tests at  $10^{-3}$  and  $10^{-4} \text{ s}^{-1}$  were performed as well as strain rate change tests between these rates.

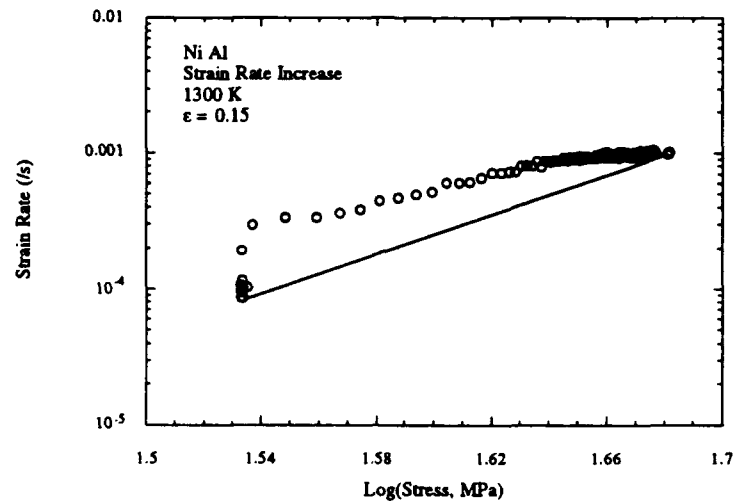
Figure 2 shows the results of the strain rate change tests between  $10^{-3}$  and  $10^{-4} \text{ s}^{-1}$ . NiAl shows pure metal like (Class II) behavior as evidenced by both the strain rate increase and strain rate decrease. During a strain rate increase, the intermetallic seems initially soft and moves above the steady state line; during the rate decrease, it appears hard. The constant structure stress exponent is of the order 100 compared with the steady state stress exponent of 6.6. Whittenberger<sup>[2]</sup> measured a stress exponent of 6.50 for Ni-49.94 Al at 1300 K.

The flow stress of NiBe is also found to be about 2.5 times greater than NiAl at 1300 K; nonetheless, NiBe exhibits similar pure metal behavior during strain rate change tests (Fig. 3). The stress exponent of NiBe is found to be 5.7 and the constant structure stress exponent at these temperatures is of the order 250.

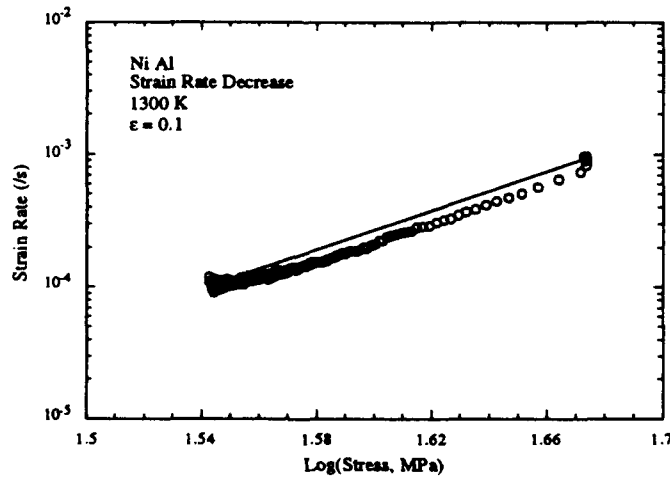
Strain rate change tests on NiAl and NiBe reveal that deformation is controlled strongly by dislocation structure. However, these transients are not as sharp as would be found for a



metal such as pure Al in which deformation is controlled exclusively by dislocation structure. Deformation in NiAl and NiBe, though dependent on the formation of a dislocation sub-structure, is also limited by the mobility of dislocations. The sluggishness of dislocation motion in NiAl is studied further below in single crystals.

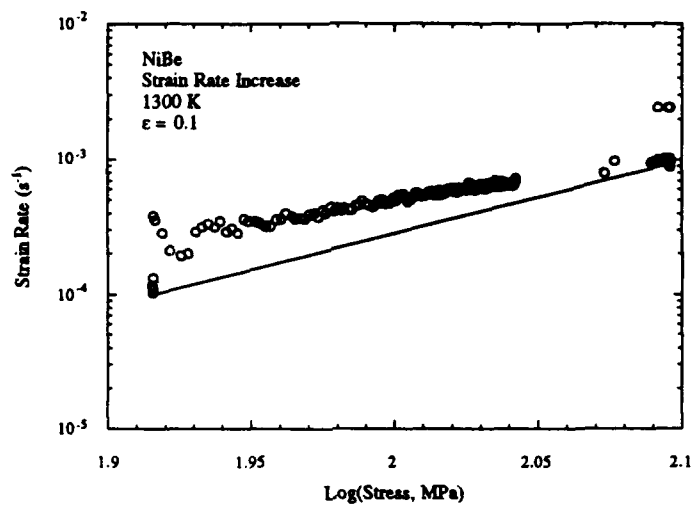


a)

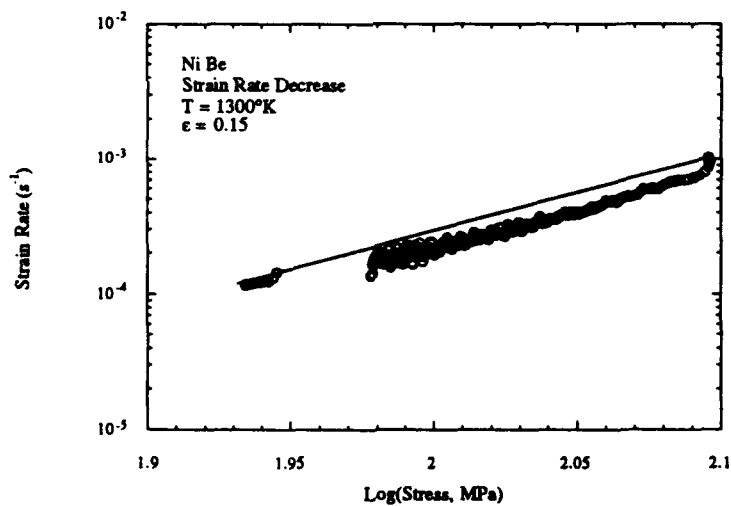


b)

**Figure 2:** Transient Response of NiAl during a) a strain rate increase and b) decrease.



a)



b)

**Figure 3:** Transient response of NiBe during a) a strain rate increase and b) decrease at 1300 K.

### References

1. D. L. Yaney, J. C. Gibeling and W. D. Nix, *Acta Metall.* **35**, 1391 (1987).
2. J.D. Whittenberger, *J. Mater. Sci.* **22**, 394 (1987).

### C. High Temperature Deformation of Single Crystal NiAl

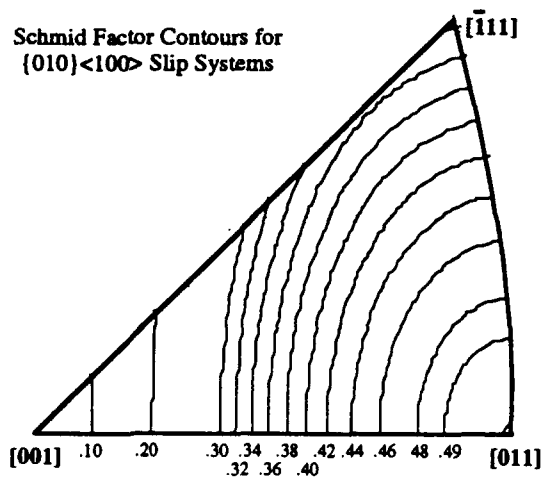
Since NiAl in polycrystalline form is brittle at low temperatures, technical application will most likely utilize single crystals. Single crystals also provide a method by which individual slip systems can be studied, to better understand dislocation mechanisms. Since NiAl has only limited slip systems, a large anisotropy in plastic deformation is expected in testing crystals with various orientations.

Dislocations in NiAl typically have a Burgers vector along the cube edge, the shortest translation vector which will preserve the B2 structure. This  $\langle 100 \rangle$  Burgers vector is illustrated in Fig. 1 of Section C as the translation of an Al atom from one well in the plane of Ni atoms to the next closest. The  $\langle 001 \rangle$  Burgers vectors in NiAl operate primarily on  $\{001\}$  planes, although  $\{011\}\langle 001 \rangle$  slip systems have been observed in some orientations<sup>[1-3]</sup>. These slip systems produce only three independent slip systems. The limited number of slip systems does not allow for arbitrary grain shape changes and is responsible for the low ductility of polycrystalline NiAl.

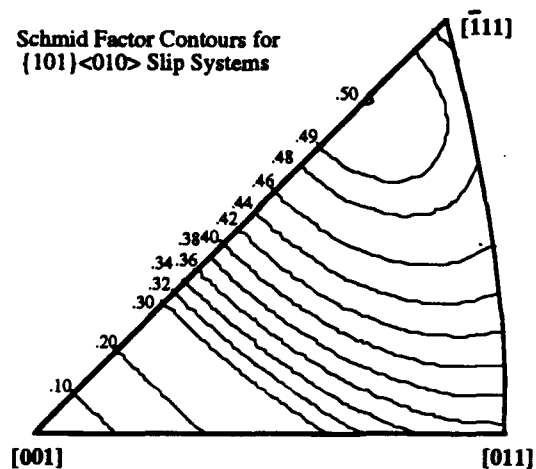
A large anisotropy in the yield properties of NiAl is also related to the limited number of slip systems. The Schmid factor describes the resolved shear stress on a slip system due to an oriented applied load. Schmid factors vary from 0 when the applied load is oriented so that no stress is resolved on the slip system, to 0.5 when the orientation provides the maximum driving force for slip. The Schmid factor for the  $\{001\}\langle 001 \rangle$  slip system has been calculated for various orientations of the applied stress and plotted as contours in Fig. 1. The maximum Schmid factor for this slip system occurs for loading along the  $[011]$  axis and a Schmid factor of zero is present for loading along the  $[001]$  axis. Plastic deformation with a  $[001]$  tensile axis would be extremely difficult since there is no resolved stress on any slip system. The "hard"  $[001]$  direction would have a higher yield strength than the "soft"  $[011]$  direction where the maximum resolved shear stress is exerted on two slip systems. Though  $\{001\}\langle 001 \rangle$  is the preferred slip system in NiAl, the  $\{011\}\langle 001 \rangle$  system also operates; its Schmid factor contours are shown in Fig. 2. Again the  $[001]$  direction is confirmed as the hard direction where slip is expected to be extremely difficult.

Figure 3 illustrates the loading axes of the samples in this investigation. The samples labeled A are within two degrees of the hard  $[001]$  loading axis. Samples in the B  $[223]$  and D  $[111]$  orientations are selected to study slip with  $\{011\}\langle 001 \rangle$  systems. All three of these slip systems will be activated equally in samples loaded along the D  $[111]$  axis; the B  $[223]$  axis is selected to preferentially activate only one slip system. Samples in the C orientation are  $10^\circ$  from  $[011]$  and are expected to activate two  $\{001\}\langle 001 \rangle$  slip systems. The hard oriented A samples have the lowest Schmid factors and thus the highest creep strength.

At room temperature, the critical resolved shear stress for slip on  $\{011\}\langle 001 \rangle$  has been measured to be slightly higher than that for slip on  $\{001\}\langle 001 \rangle$ <sup>[4]</sup>. Thus the C samples should be somewhat weaker in yielding than the B and D samples. This is confirmed with yielding experiments of Loretto in which  $[011]$  oriented samples have a lower flow stress than  $[111]$  samples. The Schmid factor for all dislocations with  $\langle 100 \rangle$  Burgers vectors is



**Figure 1:** Schmid Factor Contours for the slip system  $\{010\}\langle 100 \rangle$



**Figure 2:** Schmid Factor Contours for the slip system  $\{101\}\langle 010 \rangle$

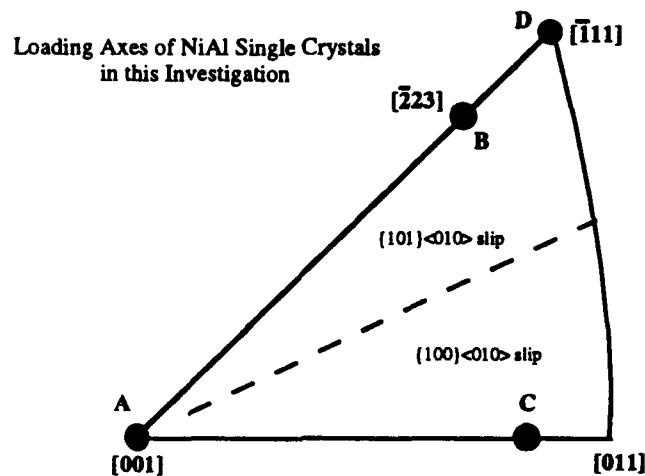


**Figure 3:** A stereographic triangle showing the four loading axes (A, B, C and D) used in this investigation.

zero for the A  $[001]$  oriented samples. Higher order Burgers vectors must be activated in this orientation for glide to occur. Samples compressed in the hard orientation have been seen to utilize the  $\langle 011 \rangle \{011\}$  slip system in yielding.

Analysis of Schmid factors assume that deformation is an athermal process driven by the applied stress resolved onto the slip system. Although this approach is appropriate for the high loads and strain rates in yielding experiments, during high temperature creep the thermal motion of dislocations is important. Dislocation climb and recovery are limited by diffusion which is enhanced in creep tests by higher temperatures and lower strain rates. As a result, the dislocation mechanisms controlling deformation during high temperature creep may differ from those controlling yielding.

Diffusion in NiAl has not been completely characterized since tracer measurements of Al are difficult. The activation energy for Ni diffusion in NiAl has been measured as 310 kJ/mole<sup>[5]</sup>. Diffusion in other B2 intermetallics has shown that diffusion of the two species in the compound differ in rate by less than a factor of two<sup>[6]</sup>. Thus we expect the activation energy for diffusion of Al in NiAl to be virtually identical to that for Ni in NiAl.

### **Orientation Dependence of the Steady State Strain Rate**

Single crystals of NiAl have been tested in high temperature creep for the orientations shown in Fig. 3. The steady state creep rates are plotted in Fig. 4 as a function of stress for each of these orientations at 1200° C. The stress exponents determined from the slopes in this plot are near 4 for the A, B and C samples (The stress exponent has not been measured for the D samples). Polycrystalline samples have also have a stress exponent near 4 when deformed at 1200° C<sup>[2]</sup>. The strength of polycrystalline NiAl is within the range of the B, C and D samples. The hard oriented A orientation has a creep rate about 100 times slower than the various soft orientations at the same applied stress. The steady state creep rate of A and B samples at 850 and 1000° C is plotted in Fig. 5. Again the hard oriented samples are significantly stronger, having a creep rate almost 100 times slower. The stress exponents are similar for the two orientations and are near 11.5 at 850° C and 4.5 at 1000° C. The stress exponent for polycrystalline NiAl in deformed at constant strain rate does not vary as much with temperature being near 6 at 850° C and 5 at 1000° C<sup>[2]</sup>.

The creep strength of NiAl loaded along [111] is found to be less than when loaded along [011]. This is in contrast with measurements of the room temperature yield strength, where [111] oriented crystals are stronger than [011] crystals. The results of the yield tests are in agreement with the predictions of the Schmid factor analysis, which determines the activated slip system. Since deformation during creep does not follow this analysis, other dislocation processes must be considered.

The softest orientation tested is 111]. This loading axis should activate three slip systems equally, which would interact to form a dislocation structure. The B [223] samples should preferentially activate one slip system and would not be expected to form an extensive dislocation structure. Yet, the [223] oriented samples, apparently without a dislocation structure, are stronger than the [111] samples.

The activation energies for creep, for samples loaded along both [001] and [223], have been determined at 1200° C. The plots of steady state strain rate versus the reciprocal of

temperature in Fig. 6 yield an activation energy of  $359 \pm 66$  kJ/mole for NiAl crystals tested along the [001] direction and  $184 \pm 37$  kJ/mole for those tested along [223]. The activation energies are not corrected for the elastic modulus but since this modulus does not vary strongly with temperature, the correction would not have a significant effect. The activation energy for the [001] crystals compares well with the activation for diffusion in NiAl suggesting that deformation is controlled by diffusion. The activation energy for the [223] crystals is much lower suggesting that an athermal glide mechanism contributes to deformation. These results suggests that the motion of  $\langle 001 \rangle$  dislocations dominates plastic flow in both hard and soft orientations. Since these dislocations have no resolved shear stress to produce glide in [001] oriented samples, they can move only by climb, so that diffusion would be expected to limit deformation. In soft orientations,  $\langle 001 \rangle$  dislocations have a resolved stress for glide.

Pascoe and Newey have measured an activation energy for yielding of NiAl crystals loaded along [001] that is a strong function of temperature<sup>[7,8]</sup>. By comparison, the activation energy for polycrystal samples is constant with temperature. In their single crystal data the activation energy increases linearly from 390 kJ/mole at 500° C to 870 kJ/mole at 1000° C. No explanation is given for why the activation energy at high temperatures is so much larger than that for diffusion in NiAl (310kJ/mole).

#### Creep Curve for B [223] Oriented Crystals

Schmid factor calculations suggest that only one  $\langle 001 \rangle \{ 110 \}$  slip system should be activated in a NiAl crystal loaded along the [223] direction. A creep curve characteristic of deformation in [223] crystals is shown in Fig. 7. The strain rate is initially very large but drops rapidly during the first few seconds of deformation. The steady state creep rate is maintained through 20% strain, decreasing only slightly due to the rotation of the tensile axis during creep. Samples tested at temperatures as low as 850° C show little strain hardening, consistent with the dominant operation of one slip system.

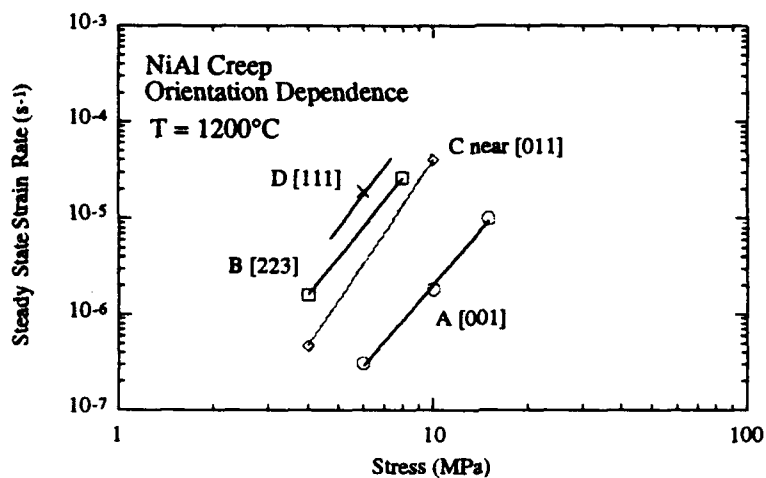


**Figure 4:** The steady state creep rate of NiAl single crystals at 1200 °C tested along the orientations labeled in Figure 3.

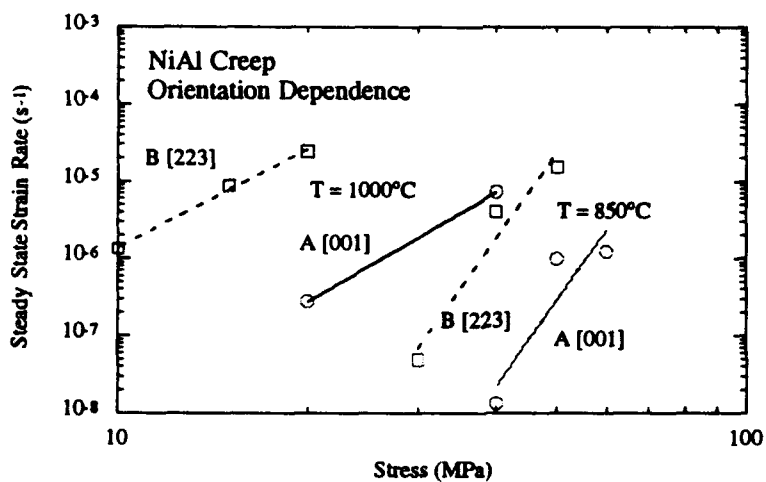
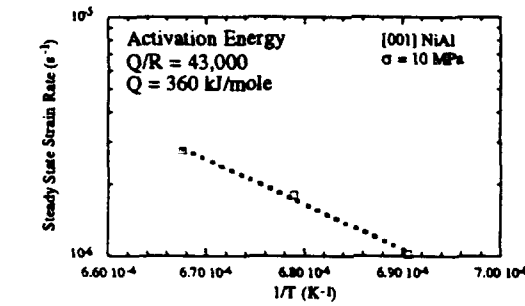
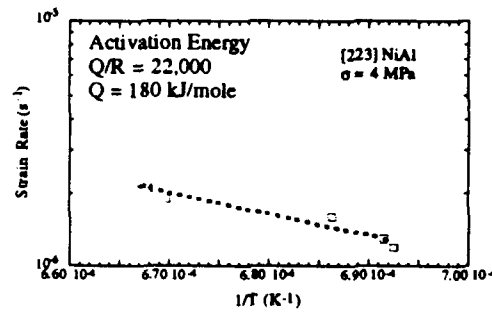


**Figure 5:** The steady state creep rate of NiAl single crystals at 850 and 1000 °C tested along the orientations labeled in Figure 3.



(a)



(b)

**Figure 6:** The steady state strain rate of NiAl single crystals at a constant stress at temperatures near 1200° C. The slope of the curves yield the activation energies for steady state creep for crystals loaded along (a) [001] and (b) [223].

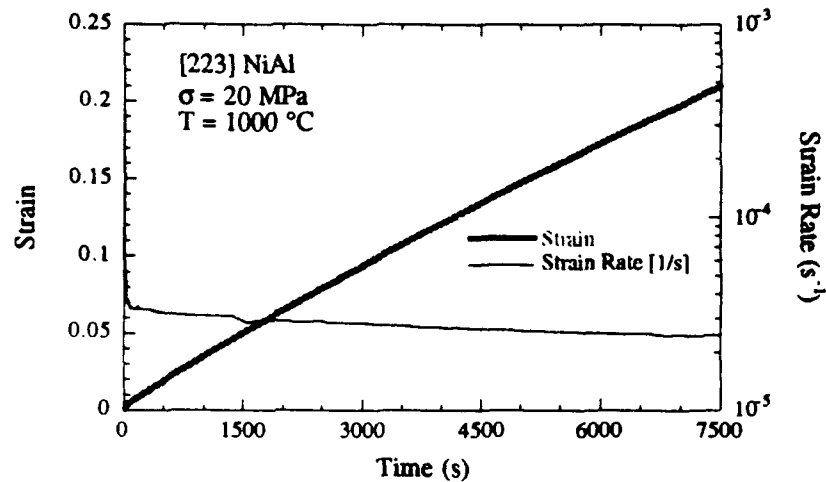


**Figure 7:** A characteristic creep curve showing both strain and strain rate as a function of time for a NiAl crystal loaded along [223].



### Creep Curve for A [001] Oriented Crystals

A characteristic creep curve for a NiAl crystal tested along the hard [001] is shown in Figure 8. This creep curve is distinct from that for the [223] direction in both the initial transient and the long term strain hardening. The initial transient in the [001] creep curve (Fig. 8(b)) is characterized by a strain rate which is initially low and rises to a maximum before decreasing to the steady state value. This sigmoidal behavior is characteristic of a material with a very low initial mobile dislocation density<sup>[9]</sup>. Deformation in the crystal is initially low, being limited by the mobility of the few mobile dislocation. The strain rate,  $\dot{\epsilon}$ , is given by the product of the dislocation density,  $\rho_m$ , the Burgers vector,  $b$  and the dislocation velocity,  $v$ :

$$\dot{\epsilon} = \rho_m b v \quad (1)$$

As deformation continues, additional mobile dislocations are created or activated as described by the breeding constant  $\delta$ :

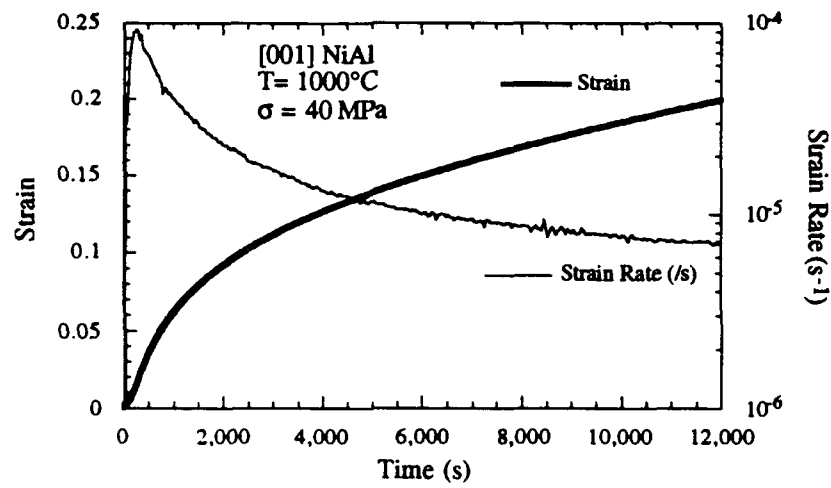
$$\dot{\rho}_m = \rho_m v \delta \quad (2)$$

The velocity of mobile dislocations depends on the effective stress,  $\tau_{eff}$ , and the temperature  $T$ :

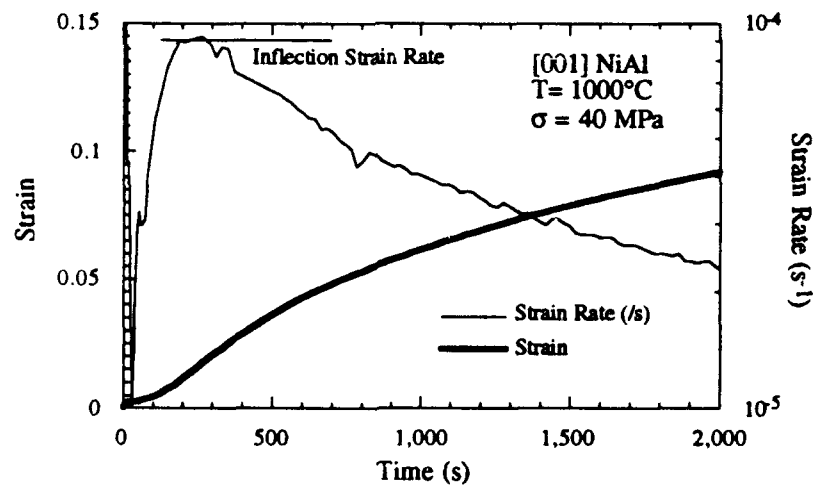
$$\begin{aligned} v &= v_0 (\tau_{eff})^m \exp (-Q/RT) \\ \tau_{eff} &= (\tau_{app} - \alpha \sqrt{\rho_m}) \end{aligned} \quad (3)$$

The effective stress includes both the applied stress,  $\tau_{app}$ , and the long range stress from neighboring dislocations. As the number of dislocations increases, the back stress built up in the crystal lowers the velocity of the mobile dislocations. The sigmoidal behavior results from this competition between increasing mobile dislocation density and decreasing dislocation velocity. The inflection point strain rate occurs when the derivative of the strain rate with respect to time is zero. The inflection strain rate,  $\dot{\epsilon}_{infl}$ , can be calculated in this way to obtain:

$$\dot{\epsilon}_{infl} = \dot{\epsilon}_0 (\tau_{app})^{m+2} \exp (-Q/RT) \quad (4)$$



(a)



(b)

**Figure 8:** A characteristic creep curve showing both strain and strain rate as a function of time for a NiAl crystal loaded along [001]. Both (a) the full creep curve and (b) the initial sigmoidal transient are shown

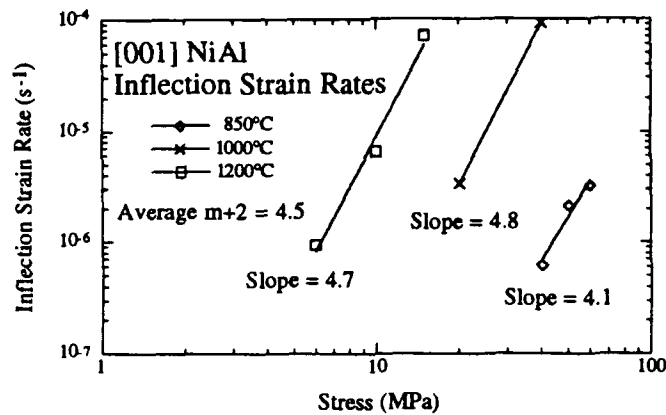


**Figure 9:** Inflection strain rate observed in NiAl crystals tested along [001] as a function of applied stress for various temperatures. The average stress exponent is 4.5.

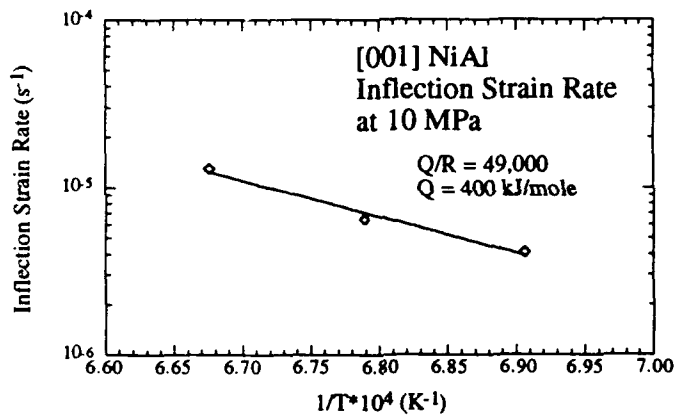


**Figure 10:** The inflection strain rate measured for NiAl crystals tested along [001] at a stress of 10 MPa.

The inflection point strain rates for samples tested along the [001] axis are plotted against the applied stress in Fig. 9 for various temperatures. The stress exponent,  $m+2$ , in Equation (4) is near 4.5 for all temperatures between 850 and 1200 °C. By contrast, the stress exponent for steady state creep (Fig. 4 and 5) varies from 4 to 11 in this temperature range. The variance of the stress exponent calculated from the inflection strain rate and that determined by the steady state strain rate in Figures 4 and 5 is a result of this structure that forms during steady state.

The activation energy of the inflection strain rate is shown in Fig. 10 to be  $405 \pm 117 \text{ kJ/mole}$ . This compares with both the activation energy of steady state creep ( $360 \text{ kJ/mole}$ ) and of diffusion in NiAl ( $310 \text{ kJ/mole}$ ). This result suggests that diffusion limits the motion of dislocations during the initial transient as well as during steady state

creep. Dislocations often must climb to overcome the obstacles presented by a steady state dislocation structure; but in hard oriented NiAl crystals, dislocations also appear to climb even at early times when no structure has formed. Sigmodial creep behavior is evident in NiAl samples tested along [001] at all temperatures between 850 and 1200° C. A slight sigmodial behavior is seen in soft samples tested along [223], but only at high temperatures and low stresses.

The steady state creep behavior for NiAl crystals tested along [001] is shown in Fig. 8(a). The creep rate at 1000° C is still decreasing after 20% strain in this crystal whereas steady state is reached within 0.5% strain for [223] oriented crystals. The extensive hardening of [001] crystals suggests that dislocation substructure, although slow to form, is important to steady state creep. Crystals tested in the hard orientation at 1200° C show less strain hardening.

#### TEM Observation of Dislocations in A [001] and B [223] Oriented Crystals

After the samples were tested, they were cooled under load to lock in the dislocation structure and then specimens were prepared to be viewed with the transmission electron microscope (TEM). Figure 11 illustrates the dislocation configuration in a NiAl crystal loaded along the [223] axis to 23% strain with a constant stress of 8 MPa at 1000° C. There are few dislocation interactions, consistent with deformation dominated by one slip system. Except for some reacted segments between dislocations, all of the dislocations in the crystal have Burgers vectors of  $\langle 001 \rangle$  though they lie on {010} planes and not {110} planes as suggested by the resolved shear stresses. Also many of the dislocations are curved, not in their slip plane, but in their climb plane suggesting that diffusion is prominent during deformation.

In contrast to the dislocations found in [223] crystals, the dislocation configurations in samples tested along [001] reveal extensive network formation and many higher order Burgers vectors. Figures 12 and 13 are indicative of the dislocation networks found in a NiAl crystal tested along [001] to 9% strain with a load of 20 MPa at 1000° C. Dislocations with  $\langle 110 \rangle$  and  $\langle 111 \rangle$  Burgers vectors are evident in the network in Fig. 12 although only  $\langle 001 \rangle$  Burgers vectors are found in dislocations isolated from such networks. Higher order Burgers vectors appear to be a result of interactions between dislocations and not produced by the activation of additional slip vectors. TEM analysis suggests that  $\langle 001 \rangle$  dislocations contribute greatly to deformation in crystals loaded along [001] although none of these dislocations would have a resolved shear stress to induce glide. Dislocation climb and thus diffusion must play an important role in deformation along the hard orientation.

Networks of the type shown in Figure 13 are found throughout the deformed crystal and creates a subgrain structure within the crystal. This network consists of an ordered arrangement of two types of 45° dislocations with different  $\langle 001 \rangle$  Burgers vectors. The spacing of dislocations in this network and the subgrain size both vary with the applied stress. In samples tested at 1000° C the steady state subgrain size is 100 to 200  $\mu\text{m}$  with an applied stress of 20 MPa and 10 to 20  $\mu\text{m}$  with a stress of 40 MPa. The substructure

shown in Figure 13 is that associated with the steady state deformation in the experiment shown in Figure 8 (a).



**Figure 11:** A TEM micrograph of dislocations in NiAl crystals deformed along a  $[223]$  direction. Little dislocation interactions is observed.

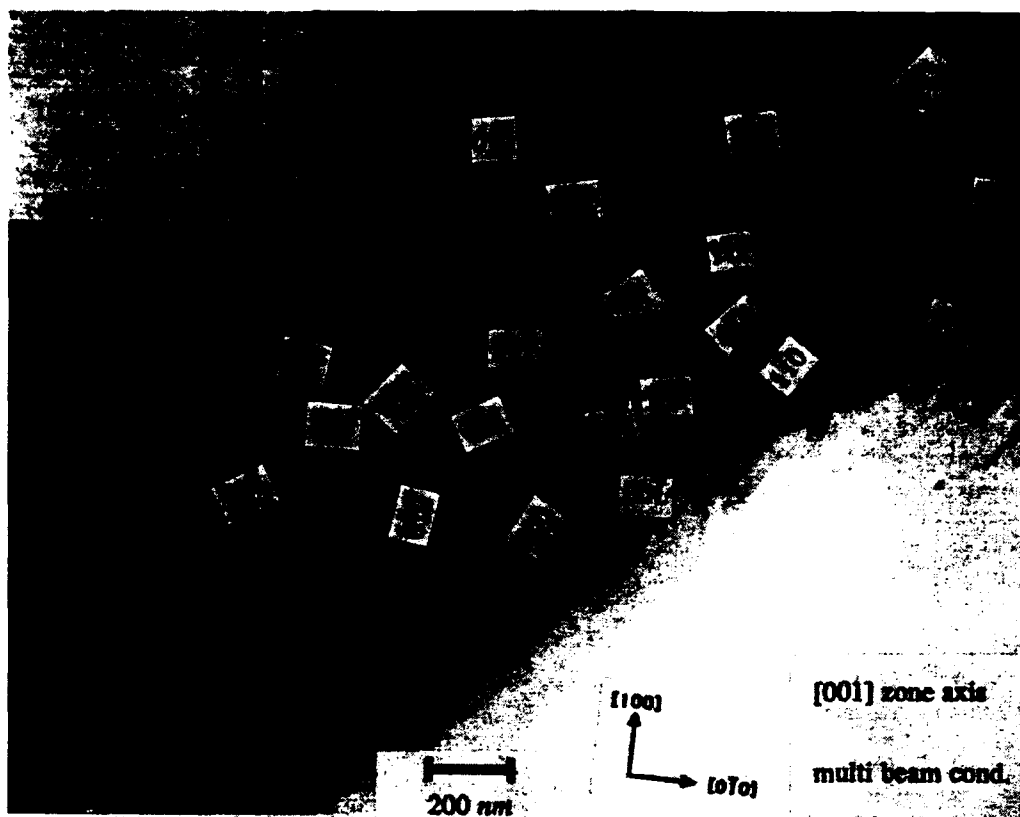


**Figure 12:** A TEM micrograph of a dislocation network in a NiAl single crystal deformed along a  $[001]$  direction. High order Burgers vectors are seen as a result of dislocation interactions.

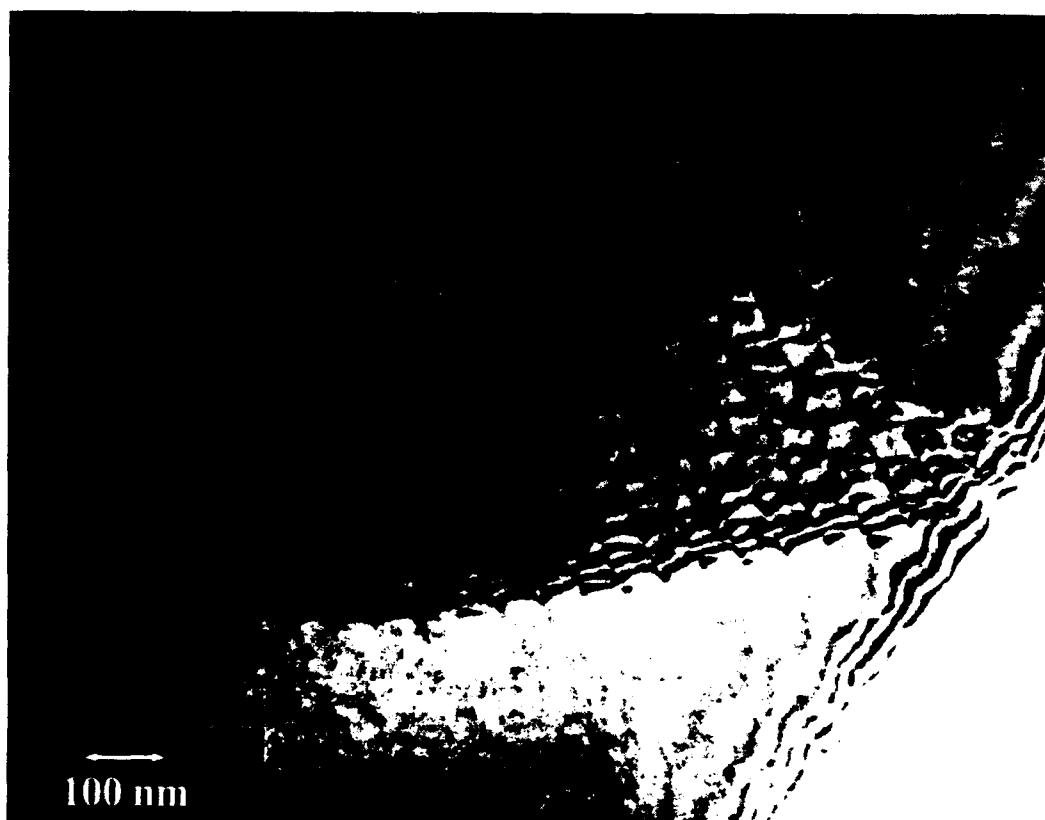
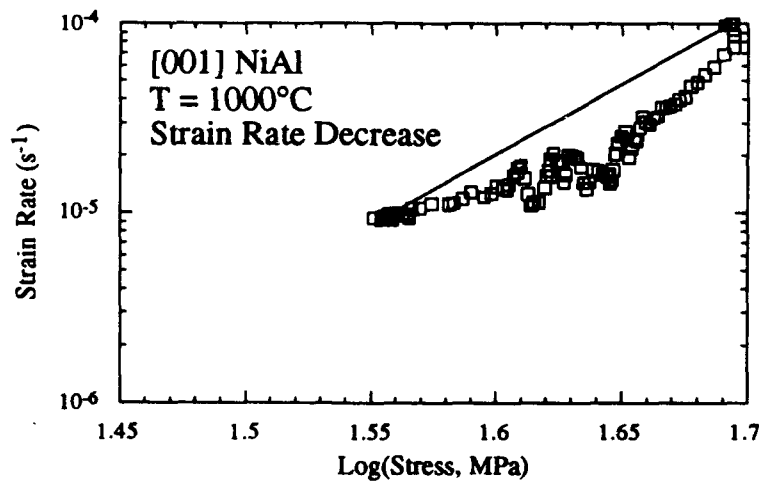


**Figure 13:** A TEM micrograph of a regular network of  $\langle 001 \rangle$  dislocations in a single crystal of NiAl tested along the  $[001]$  direction.

### Transient Deformation Tests on [001] Oriented Crystals

The transient associated with a rapid strain rate increase or decrease is useful in characterizing the contributions of dislocation-structure and dislocation-mobility controlled deformation. Polycrystalline NiAl has been studied with strain rate change experiments, as explained in Section C. The results of polycrystalline experiments indicate that dislocation motion is sluggish but nonetheless controlled by a dislocation substructure. Transient tests have also been performed on single crystals loaded along the [001] orientation.

A strain rate decrease experiment for a NiAl crystal oriented along [001] is shown in Figure 14(a). The data points the line defining steady state flow, suggesting that dislocation sub-structure is important. As with the polycrystalline transient, the degree of deviation from the equilibrium line is much smaller than that for a pure metal like Al. A strain rate increase experiment is shown in Fig. 14(b). It reveals structure controlled deformation though more weakly than true pure metal behavior. Transient tests on [001] oriented crystals suggest that a structure, such as shown in Figure 13, limits deformation and also that dislocation motion is sluggish in this orientation.



(a)

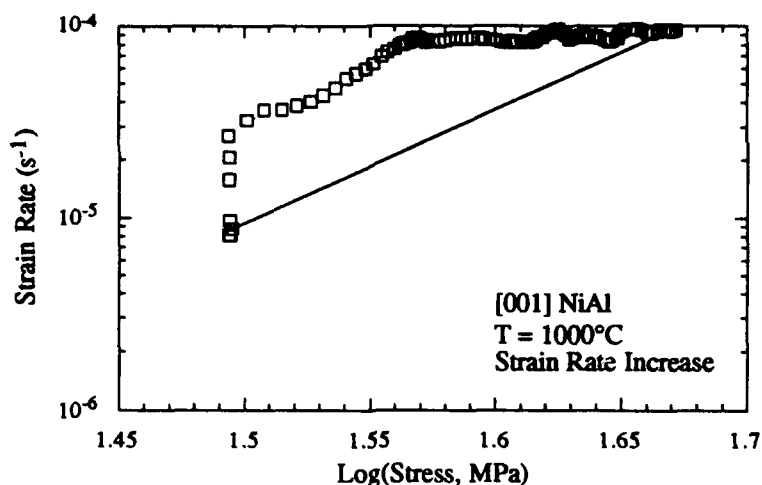


**Figure 14:** The transients associated with a (a) strain rate decrease and (b) strain rate increase for a NiAl single crystal loaded along [001].

### Conclusions

Plastic flow in NiAl is highly anisotropic. However, deformation in a variety of orientations appears to be controlled only by the motion of  $\langle 001 \rangle$  dislocations. Easy  $\langle 001 \rangle$  glide, however, is inhibited in crystals loaded along the hard [001] orientation. The initial creep transient of crystals in this orientation is characterized by a low number of initial mobile dislocations which move by diffusive processes. Climb of  $\langle 001 \rangle$  dislocations appears prevalent in hard oriented crystals and there is no evidence of glide of dislocations with higher order Burgers vectors during high temperature creep. Glide of  $\langle 001 \rangle$  dislocations controls deformation in NiAl crystals with loading axes near [223], [001] and [111]. Because of the limited number of slip systems, single slip can be observed in samples oriented along [223]. The motion of dislocations gliding in these soft oriented samples is not as sluggish as when loaded in the hard orientation where climb is dominant.

Transient tests of hard oriented crystals reveal both structure-controlled and mobility-controlled aspects of deformation. The dislocation substructure which limits deformation has been observed with TEM and is characterized as a network of  $\langle 001 \rangle$  dislocations. Dislocations with  $\langle 110 \rangle$  Burgers vectors have been observed in NiAl crystals yielded in the hard orientation but no evidence of their contribution to deformation is seen in high temperature creep tests.



## References

1. A. Ball, and R. E. Smallman, *Acta metall.* **14**, 1349 (1966).
2. R. R. Vandervoort, A. K. Mukerjee, and J. E. Dorn, *Trans ASM* **59**, 930 (1966).
3. A. Ball, and R. E. Smallman, *Acta metall.* **14**, 1517 (1966).
4. R. D. Field, D. F. Lahrman, and R. Darolia, to be published
5. G. F. Hancock and B. R. McDonnell, *Phys. Stat. Sol (a)* **4**, 143 (1971).
6. M. Koiwa.
7. R. T. Pascoe and C. W. A. Newey, *Metal. Sci. J.* **2**, 138 (1968)
8. R. T. Pascoe and C. W. A. Newey, *Metal. Sci. J.* **5**, 50 (1970)
9. P. Haasen, *Dislocation Dynamics*, (eds. A. R. Rosenfield, G. T. Hahn, A. L. Bement, R. I. Jaffe) p.701, McGraw-Hill (1967).

### III. Particle Strengthening of Intermetallic Alloys

#### A. High Temperature Compression Tests of $\text{Ni}_3\text{Al}-\text{Al}_2\text{O}_3$ Composites

K. R. Forbes (Graduate Research Assistant)

The technical demands of high temperature structural components has stimulated the development of intermetallic compounds which are able to maintain high strengths at elevated temperatures.  $\text{Ni}_3\text{Al}$  has been successfully used in selected intermediate temperature applications but is still not appropriate for higher temperatures. The variation in strength of a  $\text{Ni}_3\text{Al}$  (Hf, B) alloy with temperature is shown in Figure 1. The strength of the alloy is maximum at about  $750^\circ\text{C}$  but falls rapidly above this temperature. It is this rapid decrease in strength that disqualifies  $\text{Ni}_3\text{Al}$  for high temperature applications.

Ceramic materials, on the other hand, have very high melting temperatures and can maintain their strength to temperatures much above that of intermetallics. The strength of single crystal  $\text{Al}_2\text{O}_3$  is compared with the strength of  $\text{Ni}_3\text{Al}$  at various temperatures in Figure 1. Ceramics, however, are extremely brittle and thus inappropriate for many high temperature applications. A more ideal material would combine the ductility and strength of  $\text{Ni}_3\text{Al}$  with the high temperature integrity of a ceramic. A composite of  $\text{Ni}_3\text{Al}$  and a ceramic is the most direct approach to realizing the benefits of both in one material. The purpose of

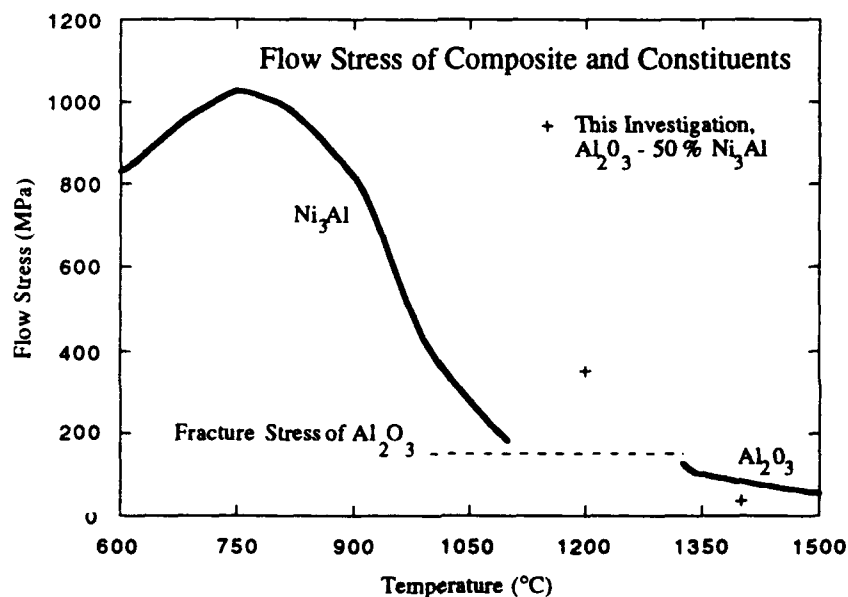


**Figure 1:** Comparison of the Flow Stress of  $\text{Al}_2\text{O}_3 - \text{Ni}_3\text{Al}$  Composite and its Constituents. 0.2% Offset Yield Strength of  $\text{Ni}_3\text{Al}$  from [1]. Yield Strength of Single Crystal  $\text{Al}_2\text{O}_3$  from [2].

this investigation is to explore the enhancements offered by a  $\text{Ni}_3\text{Al}-\text{Al}_2\text{O}_3$  composite over the properties of the individual constituents.

The composites for this study were provided by the Research and Development Division of the Lockheed Missiles and Space Company. The composites were made from mixtures of  $75\text{ }\mu\text{m}$  particles of  $\text{Ni}_3\text{Al}$  (Hf,B) and  $75\text{ }\mu\text{m}$  particles of  $\text{Al}_2\text{O}_3$  at weight fractions of  $\text{Ni}_3\text{Al}$  equal to 0.17, 0.32 and 0.50. The mixtures were consolidated by hot pressing in a vacuum for 2 hours at  $1200^\circ\text{C}$  under a 200 MPa load. Cylindrical samples, 4.5 mm diameter by 9 mm length, were cut from the pressed ingot.

The intermetallic composite samples were tested at room temperature and at 1200 and  $1400^\circ\text{C}$ . A constant compressive strain rate of  $10^{-4}\text{ s}^{-1}$  was imposed while the load and displacement at the sample were measured. Elastic properties could not be measured during these compression tests; so, instead of more a typical representation of yield strength, the flow stress at 2% strain was used for comparison of the sample strengths. The stress-strain curves for these compression tests are show in Figure 2 and the value of the 2% offset yield strength are recorded in Table 1.

As expected, the composite has increased high temperature strength compared to  $\text{Ni}_3\text{Al}$  but lower strength than  $\text{Al}_2\text{O}_3$ . The strength of  $\text{Al}_2\text{O}_3$  is significantly reduced with an addition of only 17 weight per cent  $\text{Ni}_3\text{Al}$ . Increasing the weight fraction of  $\text{Ni}_3\text{Al}$  to 32 per cent results decreases the strength of the composite insignificantly. The sample of 0.50 weight fraction  $\text{Ni}_3\text{Al}$ , however, has a greater strength then either of the samples with lower compositions. This is surprising since adding more of the lower strength  $\text{Ni}_3\text{Al}$  to the composition would suggest that the strength should decrease further. The 0.50 weight fraction composite also keeps much of its strength even to  $1400^\circ\text{C}$  which is slightly above the melting temperature of  $\text{Ni}_3\text{Al}$  ( $T_m = 1395^\circ\text{C}$ ).

**Table 1.** The 2% offset yield strength of  $\text{Ni}_3\text{Al} - \text{Al}_2\text{O}_3$  composites at various test temperatures.

<u>Test temperature</u>	<u>Weight Fraction of <math>\text{Ni}_3\text{Al}</math> in Composite</u>		
	<u>0.17</u>	<u>0.32</u>	<u>0.50</u>
27° C	fracture (300 MPa)	fracture (225 MPa)	fracture (300 MPa)
1200° C	120 MPa	110 MPa	350 MPa
1400° C	16 MPa	16 MPa	37 MPa

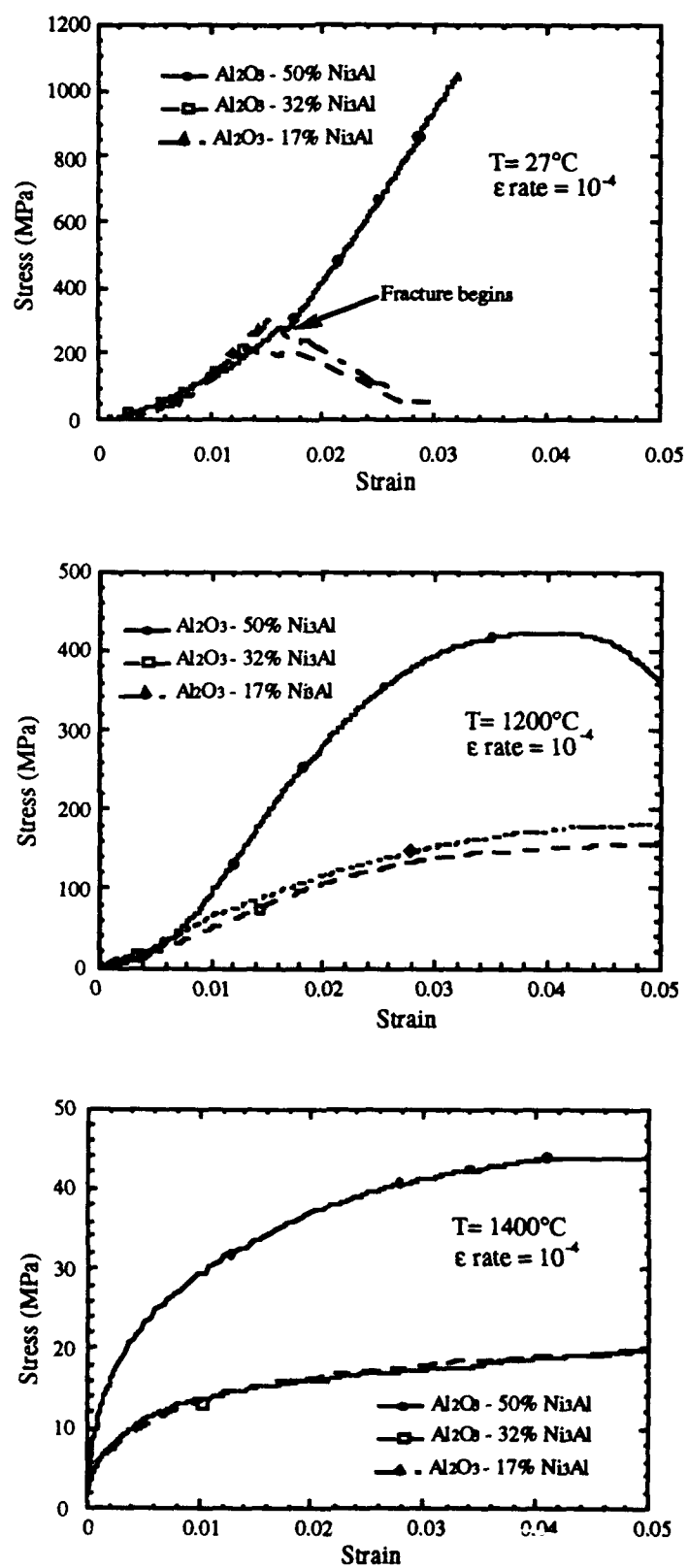


**Figure 2:** Stress-strain plots for  $\text{Ni}_3\text{Al}$  -  $\text{Al}_2\text{O}_3$  composites at various temperatures.

The strength of the higher weight fraction samples suggests that larger fractions of  $\text{Ni}_3\text{Al}$  promote an additional phase between  $\text{Al}_2\text{O}_3$  and  $\text{Ni}_3\text{Al}$ . Whereas small additions of  $\text{Ni}_3\text{Al}$  to  $\text{Al}_2\text{O}_3$  results in a decrease in strength due to the weakening of the bonding between  $\text{Al}_2\text{O}_3$  grains, an additional phase, if present, could somewhat strengthen the bonding between the ceramic grains. This postulation has yet to be tested by a more complete analysis of the composition of the matrix surrounding the ceramic grains.

The ductility of the composite, however, is much improved over that of the  $\text{Al}_2\text{O}_3$ . The ceramic fractures before yielding at temperatures below  $1300^\circ\text{C}$  but the composites show no tendency to fracture except in the room temperature tests. Even the higher strength 0.50 weight fraction sample shows no loss of ductility.

In Figure 1, the yield strength of the strong 0.50 composite is plotted along with the strengths of  $\text{Ni}_3\text{Al}$  and single crystal  $\text{Al}_2\text{O}_3$ . The strength of the composite is greater than that of the intermetallic component though less than that of the ceramic component; and its ductility is much increased over the ceramic. Thus,  $\text{Ni}_3\text{Al}-\text{Al}_2\text{O}_3$  composites show promise for high temperature applications although at present the strengthening mechanisms are not well understood.

#### References

1. R. S. Bellows and J. K. Tien, *Scripta Metall.* **21**, 1659 (1987).
2. M. L. Kronberg, *J. Am. Ceram. Soc.* **45**, 274 (1962).

## **B. High Temperature Compression Tests of $\text{Ni}_3\text{Al}-\text{Y}_2\text{O}_3$ Particulate Composites**

D. D. Sternbergh (Graduate Research Assistant)

### Introduction

Its increasing strength with temperature has made  $\text{Ni}_3\text{Al}$  an attractive material for structural applications at intermediate temperatures. However, the yield strength reaches a maximum around  $750^\circ\text{C}$ ; above this point it drops sharply with temperature. Dispersion strengthening has been used successfully in a number of materials to help maintain mechanical strength at high temperatures. We are investigating the effects of oxide dispersoids on the strength of intermetallic  $\text{Ni}_3\text{Al}$  at intermediate and high temperatures.

Our model system is  $\text{Ni}_3\text{Al}$  containing a fine, uniform dispersion of yttrium oxide particles. A microstructure of this kind is difficult or impossible to achieve by conventional melting and solidification techniques. For this reason these materials are usually prepared using solid state and powder metallurgical processing techniques. We have prepared these materials by mechanical alloying, a solid state processing technique developed for producing composite metal powders with controlled, extremely fine microstructures.

The materials were prepared from pre-alloyed powders, kindly supplied by Dr. C.T. Liu of Oak Ridge National Laboratories, with a composition  $\text{Ni}-22.3\text{ Al}-0.51\text{ Zr}-0.09\text{ B}$ , an alloy named IC-50. The powder was mechanically alloyed with yttria particles, consolidated in vacuum, and extruded. Compression samples were tested using the testing apparatus described in section I.

### Microstructure

These materials retained an ultra-fine grain structure. Individual grains could not be resolved optically; transmission electron microscopy revealed the grains to be fairly uniformly equiaxed with diameters between  $0.25-0.5\text{ }\mu\text{m}$  (see Figure 1). The yttria particles were very fine, with diameters around  $100\text{ nm}$ , and evenly distributed throughout the material.

Material tested in compression at  $1000^\circ\text{C}$  showed little change either in grain size or aspect ratio, and no observable particle coarsening. Bands of enlarged grains with no oxide particles were observed (see Figure 2); the bands were one grain wide (about  $1\text{ }\mu\text{m}$ ) and spaced about  $5\text{ }\mu\text{m}$  apart. These bands, seen in foils of tested material which were cut along the extrusion direction (and therefore containing the extrusion direction), were not observed in foils of the as-extruded material which had been cut perpendicular to (and therefore did not contain) the extrusion direction.

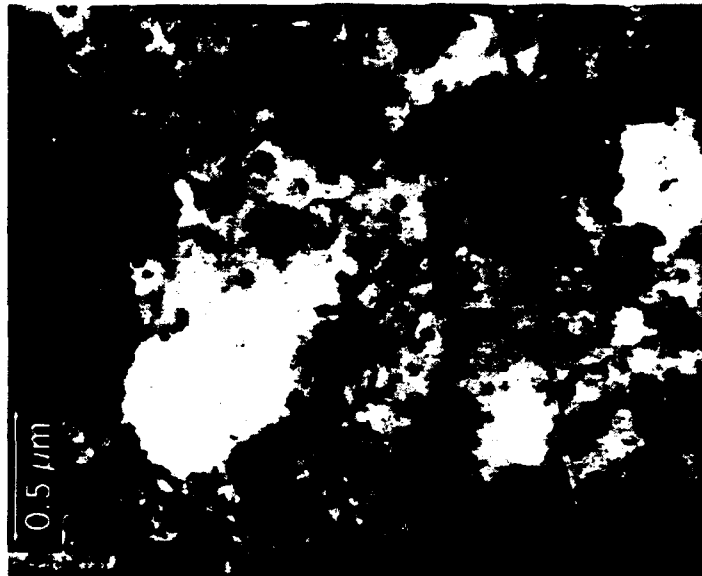


**Figure 1:** TEM micrograph of the  $\text{Ni}_3\text{Al}$  (IC-50)/ $\text{Y}_2\text{O}_3$  material, as-extruded. The plane of the film is perpendicular to the extrusion direction.

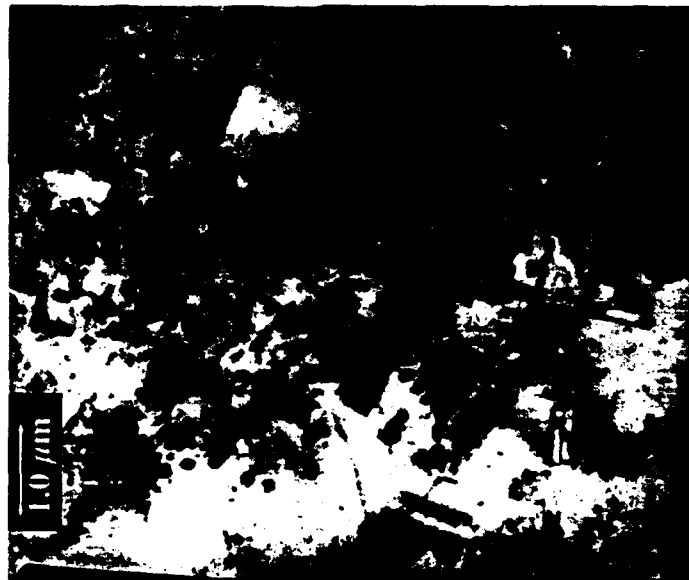


**Figure 2:** TEM micrograph of a sample after straining to 20% at 1000° C. Bands of dispersoid-free grains run horizontally across the top and bottom of the picture.

### High Temperature strength

The flow stresses at 1000° C measured at various strain rates are significantly lower than the rate-dependent stresses measured in similar alloys by Hemker<sup>[1]</sup>, Flinn<sup>[2]</sup>, and Nicholls and Rawlings<sup>[3]</sup> (see Figure 3). Hemker tested single crystals of  $\text{Ni}_3\text{Al}$  alloyed with Hf and B in tension creep, yet even accounting for the known strengthening effects of Hf at high temperatures, the strength of the ultra-fine grained material is still significantly weaker. Flinn, who did not report the microstructure of his Ni-20 at.% Al-10Fe samples,

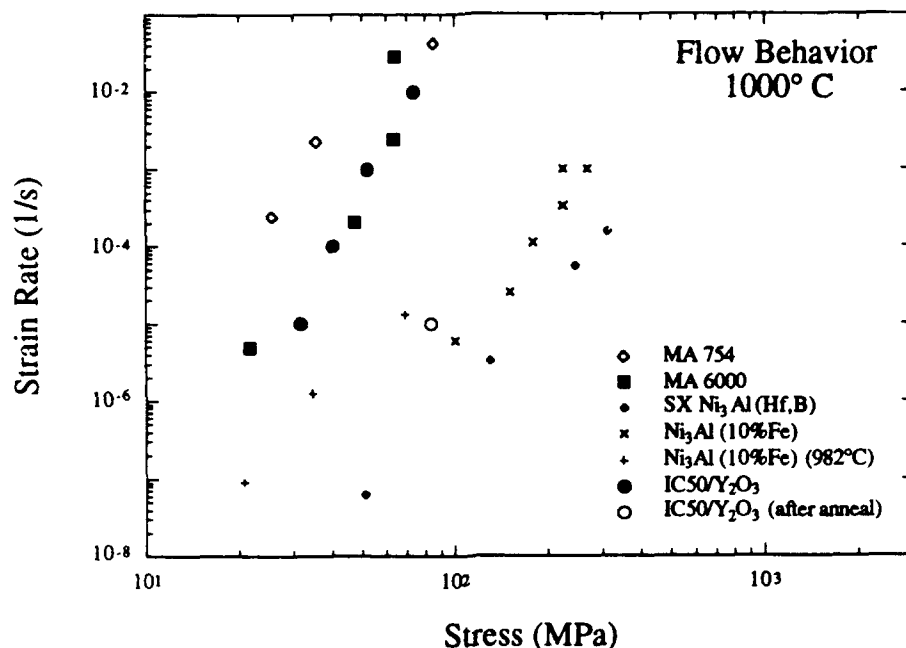


**Figure 3:** Comparison of the flow behavior of a number of high temperature materials: MA754 and MA6000 (Gregory)<sup>[4]</sup>, single crystal Ni<sub>3</sub>Al (Hf,B) (Hemker)<sup>[1]</sup>, Ni-20 Al-10 Fe (Flinn)<sup>[2]</sup>, and Ni<sub>3</sub>Al-2.5 vol% Y<sub>2</sub>O<sub>3</sub> (current study). Ultra-fine-grained Ni<sub>3</sub>Al/Y<sub>2</sub>O<sub>3</sub> is most similar to the ultra-fine-grained  $\gamma'$ -containing MA6000. After annealing, the strength approaches other Ni<sub>3</sub>Al alloys.

observed strengths five times higher. We attribute the decrease in strength which we observed to the extremely fine grain size and the contribution of grain boundary sliding to straining. Figure 4 compares the initial strength of a sample deformed at a rate of  $10^{-5}$ /s, and the same sample deformed at the same strain rate after having been annealed at  $1350^{\circ}\text{C}$  ( $0.97 T_m$ ) for 90 minutes. The as-extruded material had a flow stress at this strain rate of 32 MPa, compared to 83 MPa for the annealed sample.

The strengths of this ultra-fine-grained dispersoid-filled material is much more comparable to those of ultra-fine-grained MA 6000<sup>[4]</sup>, a dispersion-strengthened superalloy containing a high volume fraction (50–55%)  $\gamma'$  phase.

An additional feature of this material is that even at  $1000^{\circ}\text{C}$  steady state deformation was not achieved, even at 10% strain at  $10^{-5}$ /s (see Figure 4). Hardening was observed at all strain rates, suggesting the importance of some evolving dislocation structure.

The transient behavior is particularly interesting. After an increase in strain rate, the stress increases significantly, as would be expected. After reaching a peak value, however, it begins to drop — weakening with increasing strain. Usually, if sufficient straining is



allowed, it reaches a minimum and begins to increase again, showing hardening once more at the new strain rate.

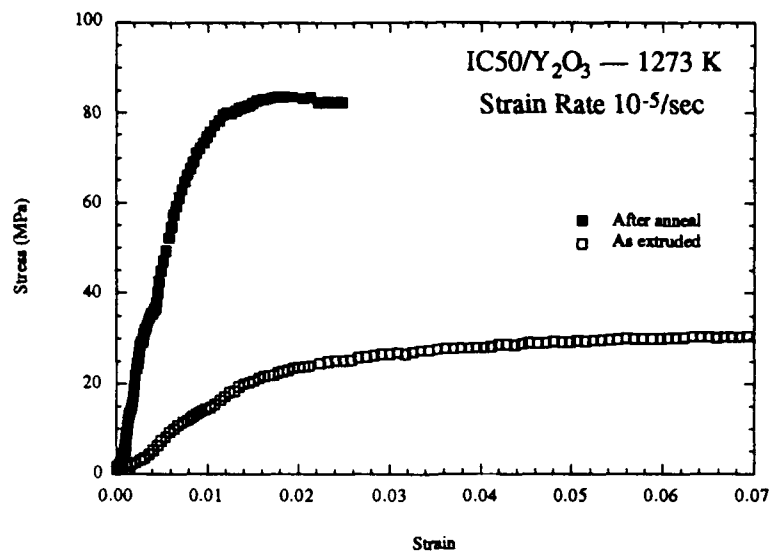


**Figure 4:** Comparison of the flow stress of IC-50/Y<sub>2</sub>O<sub>3</sub> at 1000° C and a strain rate of 10<sup>-5</sup>/s, for the material as extruded and the same sample re-tested after annealing at 1350° C for over 90 minutes.

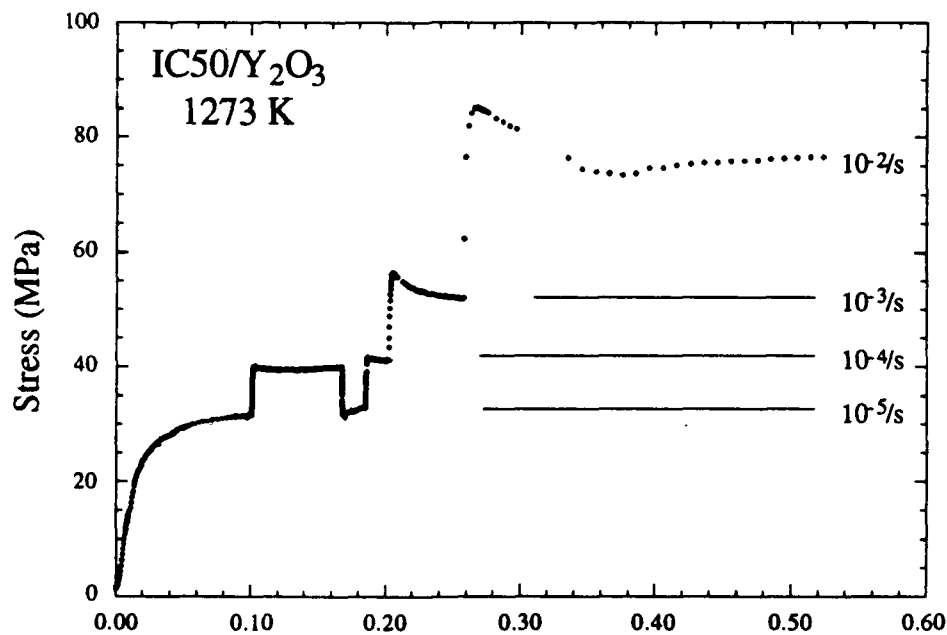


**Figure 5:** Stress-strain curve for IC-50/Y<sub>2</sub>O<sub>3</sub> at 1000° C showing several strain rate changes. Steady state is never observed, with strain hardening evident at all strain rates. The sample deformed relatively uniformly, even to 60% strain.

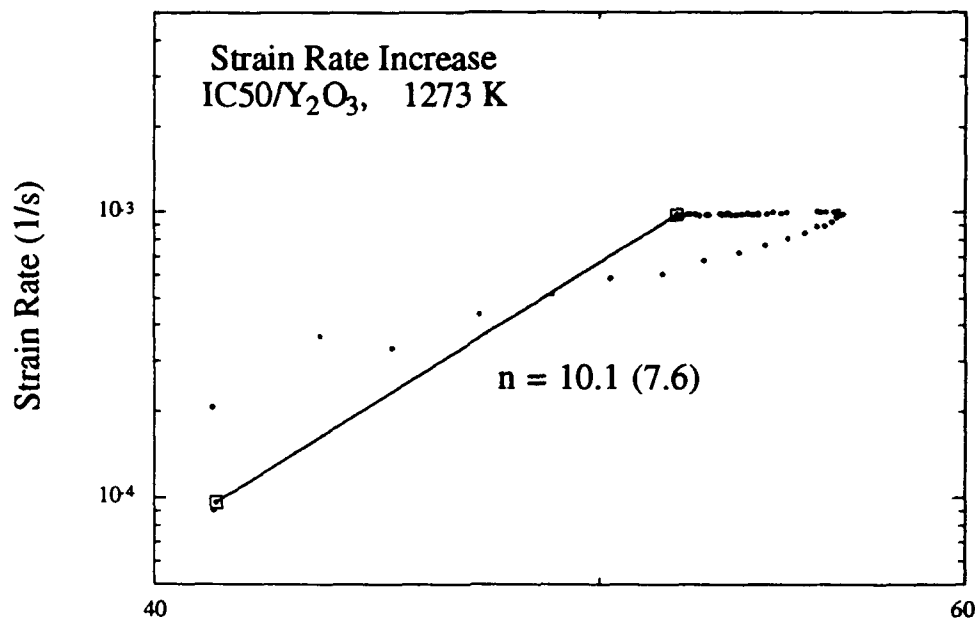


**Figure 6:** One of the strain rate transients from the test shown in Figure 4. Initially, the strain rate increases with little increase in stress, as in pure metals. At a strain rate intermediate between the original and the newly imposed rates, the stress increases dramatically to the new strain rate, at which point the sample strain softens.

Transient tests are often valuable for distinguishing clearly between materials whose deformation is controlled by the development of dislocation substructure, and those for which dislocation velocity is the controlling factor. As explained above (see section xx), materials in which dislocation substructure (Class II, or structure-controlled) is the controlling factor appear weaker than the interpolated steady-state behavior immediately following an increase in strain rate. The deformation is effected by the mobile dislocations, which constitute a small fraction of the total dislocation density. At the steady state stress associated with the slower strain rate, a critical dislocation length can be defined, below which the applied stress is insufficient to overcome the effects of curvature. Each increment of stress enables new dislocation segments to break free and run. Therefore under an increase in the imposed strain rate, a relatively small increase in stress can activate enough new dislocation segments to accommodate the increase in strain rate. As the mobile dislocations multiply, and the substructure is refined, the distribution of dislocation segment lengths decreases and the stress required to maintain the increased strain rate increases until a new steady state condition is approached.

Conversely, materials in which dislocation mobility is the controlling factor (Class I, or mobility controlled) appear stronger than the steady-state behavior immediately following an increase in strain rate. The mobile dislocations constitute a large fraction of the total dislocation density. Therefore a sudden increase in the imposed strain rate must be accommodated by driving the dislocations to run faster. This can only be accomplished by a large increase in stress. As the dislocations run at the higher velocity, however, they

multiply and the new, higher strain rate can be achieved with the dislocations running less quickly. The stress required to move the dislocations at the lower velocity is diminished, so the stress drops with continued strain until a new steady state is reached.

The transient behavior demonstrated by the dispersoid-laden  $\text{Ni}_3\text{Al}$ , however, does not demonstrate either structure-controlled or mobility-controlled features. Instead it appears to have attributes of both (see Figure 5). During a strain-rate increase, the strain rate of the sample jumps very quickly to some intermediate rate with only a very small increase in stress, after which the stress increases significantly until the new imposed strain rate is reached. At this point the stress drops off at a constant strain rate until a new "steady state" is attained. (Note that by "steady state" here is meant the stress minimum, the point at which the strain softening stops and strain hardening resumes.)

These preliminary results are not yet fully understood. They would seem to indicate the presence of some dislocations, analogous to the subcritical-length dislocations in a pure metal, which can respond quickly to a change in the imposed strain rate with only a small increase in the stress. However, this source appears to be a very limited supply; once exhausted small increments of stress are not able to activate more dislocations and large increases in the stress result from the newly imposed strain rate.

#### References

1. K. J. Hemker, Ph.D. Dissertation, Stanford University, (1990).
2. P. A. Flinn, *Trans. Met. AIME* **218**, 145 (1960).
3. J. R. Nicholls and R. D. Rawlings, *J. Mater. Sci.* **12**, 2456 (1977).
4. J. K. Gregory, Ph.D. Dissertation, Stanford University, (1983).

#### IV. Oral Presentations Resulting From AFOSR Grant No. 89-0201

1. W.D. Nix, "Advances in Understanding High Temperature Strengthening of Metals and Alloys", 1989 Edward deMille Campbell Memorial Lecture, Annual Meeting of ASM International, Indianapolis, Indiana, October 3, 1989.
2. K.J. Hemker and W.D. Nix, "Intermediate and High Temperature Creep Properties of  $\text{Ni}_3\text{Al}$  Single Crystals", Symposium on High Temperature Aluminides and Intermetallics, Fall Meeting of the Metallurgical Society, Indianapolis, Indiana, October 2, 1989.
3. K.J. Hemker, M.J. Mills and W.D. Nix, "A Critical Analysis of the Dislocation Mechanisms Associated with Yielding in  $\text{Ni}_3\text{Al}$ ", Poster Session on High Temperature Aluminides and Intermetallics, Fall Meeting of the Metallurgical Society, Indianapolis, Indiana, October 3, 1989.
4. K.J. Hemker and W.D. Nix, "An Investigation of Creep in  $\text{Ni}_3\text{Al}(\text{B},\text{Hf})$ ", Fourth International Conference on *Creep and Fracture of Engineering Materials and Structures*, Swansea, Wales, April 2, 1990.
5. W.D. Nix, K.R. Forbes and D.D. Sternbergh, "High Temperature Deformation of Intermetallic Alloys", Symposium on Physical Metallurgy of Intermetallic Compounds IV: Nickel Aluminides 1, Fall Meeting of the Metallurgical Society, Cincinnati, Ohio, October 22, 1991.

## V. Publications Resulting From AFOSR Grant No. 89-0201

1. K.J. Hemker and W.D. Nix, "An Investigation of Creep in  $\text{Ni}_3\text{Al}(\text{B,Hf})$ ", Proceedings of the Fourth International Conference on *Creep and Fracture of Engineering Materials and Structures*, Swansea, Wales, Eds: B. Wilshire and R.W. Evans, The Institute of Metals, (1990), p.51-63.
2. C.-M. Kuo, K.R. Forbes, S.P. Baker and W.D. Nix, "On the Question of Strain Rate Continuity in Stress Rate Change Experiments", *Scripta Metall.*, 24, 1623-1628 (1990).
3. K.J. Hemker, M.J. Mills and W.D. Nix, "An investigation of the Mechanisms that Control Intermediate Temperature Creep of  $\text{Ni}_3\text{Al}$ ", *Acta Metall.*, 39, 1901-1913 (1991).
4. K.J. Hemker, M.J. Mills, K.R. Forbes, D.D. Sternbergh and W.D. Nix, "Transient Deformation in the Intermetallic Alloy,  $\text{Ni}_3\text{Al}$ ", *Modelling of the Deformation of Crystalline Solids*, Eds: T.C. Lowe, A.D. Rollett, P.S. Follansbee and G.S. Daehn, The Minerals, Metals and Materials Society (1991), p. 411-421.
5. M.J. Mills, D.C. Chrzan, K.J. Hemker and W.D. Nix, "Modelling of Anomalous Flow in Intermetallic Compounds with the  $\text{L}_{12}$  Structure", *Modelling of the Deformation of Crystalline Solids*, Eds: T.C. Lowe, A.D. Rollett, P.S. Follansbee and G.S. Daehn, The Minerals, Metals and Materials Society (1991), p. 423-436.
6. K.J. Hemker, M.J. Mills, K.R. Forbes, D.D. Sternbergh and W.D. Nix, "A Description of Octahedral Glide in  $\text{Ni}_3\text{Al}$  based on Observationsw of Transient Deformation", Proceedings of the Ninth International Conference on Strength of Metals and Alloys, Eds. A. Rosen et al., Pergamon Press, 1991.
7. T.G. Nieh, K.R. Forbes, T.C. Chou and J. Wadsworth, "Microstructures and Deformation Properties of an  $\text{Al}_2\text{O}_3$ - $\text{Ni}_3\text{Al}$  Composite from Room Temperature to  $1400^\circ\text{C}$ ", (to be published in *Metall. Trans*)
8. U. Glatzel, K.R. Forbes and W.D. Nix, "Dislocation Energies in an Anisotropic Cubic Crystal: Calculations and Observations in  $\text{NiAl}$ " (to be submitted to *Phil. Mag.*)

## **VI. Ph.D. Students Supported By AFOSR Grant No. 89-0201**

1. Kevin J. Hemker  
"A Study of High Temperature Deformation in the Intermetallic Alloy  
Ni<sub>3</sub>Al"  
Ph.D. Stanford University, 1990
2. Keith R. Forbes  
Ph.D. expected in 1993.
3. D. Daniel Sternbergh  
Ph.D. expected in 1993.